Developmental Biology 374 (2013) 127–141

Contents lists available at SciVerse ScienceDirect

Developmental Biology

journal homepage: www.elsevier.com/locate/developmentalbiology

Ecdysone-dependent and ecdysone-independent programmed cell death in the developing optic lobe of *Drosophila*

Yusuke Hara [a,b], Keiichiro Hirai [a], Yu Togane [a,b], Hiromi Akagawa [a,b], Kikuo Iwabuchi [b], Hidenobu Tsujimura [a,*]

[a] Developmental Biology, Tokyo University of Agriculture and Technology, 3-5-8, Saiwai-cho, Fuchu-shi, Tokyo 183-8509, Japan
[b] Biological Production Science, Tokyo University of Agriculture and Technology, 3-5-8, Saiwai-cho, Fuchu-shi, Tokyo 183-8509, Japan

ARTICLE INFO

Article history:
Received 8 August 2012
Received in revised form
30 October 2012
Accepted 2 November 2012
Available online 10 November 2012

Keywords:
Optic lobe
Cell death
Ecdysone
EcR
FTZ-F1
Drosophila

ABSTRACT

The adult optic lobe of *Drosophila* develops from the primordium during metamorphosis from mid-3rd larval stage to adult. Many cells die during development of the optic lobe with a peak of the number of dying cells at 24 h after puparium formation (h APF). Dying cells were observed in spatio-temporal specific clusters. Here, we analyzed the function of a component of the insect steroid hormone receptor, EcR, in this cell death. We examined expression patterns of two EcR isoforms, EcR-A and EcR-B1, in the optic lobe. Expression of each isoform altered during development in isoform-specific manner. EcR-B1 was not expressed in optic lobe neurons from 0 to 6 h APF, but was expressed between 9 and 48 h APF and then disappeared by 60 h APF. In each cortex, its expression was stronger in older glia-ensheathed neurons than in younger ones. EcR-B1 was also expressed in some types of glia. EcR-A was expressed in optic lobe neurons and many types of glia from 0 to 60 h APF in a different pattern from EcR-B1. Then, we genetically analyzed EcR function in the optic lobe cell death. At 0 h APF, the optic lobe cell death was independent of any EcR isoforms. In contrast, EcR-B1 was required for most optic lobe cell death after 24 h APF. It was suggested that cell death cell-autonomously required EcR-B1 expressed after puparium formation. βFTZ-F1 was also involved in cell death in many dying-cell clusters, but not in some of them at 24 h APF. Altogether, the optic lobe cell death occurred in ecdysone-independent manner at prepupal stage and ecdysone-dependent manner after 24 h APF. The acquisition of ecdysone-dependence was not directly correlated with the initiation or increase of EcR-B1 expression.

Introduction

During development of the central nervous system, excess neurons are initially produced, then superfluous neurons die, and surviving neurons form mature neural circuits. To reveal the mechanism and the significance of this cell death is essential for understanding neural development. In the *Drosophila* optic lobe, many cells die during development (Fischbach and Technau, 1984; Hofbauer and Campos-Ortega, 1990; Togane et al., 2012). Here, we investigate the role of the insect steroid hormone, ecdysone, in this cell death.

The optic lobe processes and transmits visual information from the compound eye to the central brain. It consists of four neuropils—the lamina, medulla, lobula, and lobula plate—and surrounding cortices. During metamorphosis, the optic lobe develops from the optic lobe primordium, which includes two proliferation centers—the outer optic anlagen (OOA) and the inner optic anlagen (IOA) (Fischbach and Hiesinger, 2008; Meinertzhagen and Hanson, 1993). Lamina neurons are produced by precursor cells that receive signals from photoreceptor axons on the lateral side of the OOA (Huang and Kunes, 1998, 1996; Huang et al., 1998; Selleck et al., 1992; Selleck and Steller, 1991; Umetsu et al., 2006). Medulla neurons differentiate from neuroblasts that are produced on the medial side of the OOA under the control of several signaling pathways (Egger et al., 2010; Fischbach and Hiesinger, 2008; Meinertzhagen and Hanson, 1993; Ngo et al., 2010; Wang et al., 2011a, 2011b; Yasugi et al., 2010, 2008). T2/T3/C neurons and lobula plate neurons are derived from the IOA; however, the development of these neurons has not been described in detail. The optic lobe glia also develop during optic lobe development, and they have essential roles in the formation of neural circuits and neuropil boundaries, proliferation and survival of neurons, and functions of synapses (reviewed by Chotard and Salecker, 2007; Edwards and Meinertzhagen, 2010).

Cell death in the optic lobe occurs in a specific spatio-temporal pattern (Togane et al., 2012). It occurs in two rounds. The first round begins at the onset of metamorphosis and continues until 48 h APF. Many cells die in this round, with a peak at 24 h APF. Dying cells are distributed in specific regions of the cortices, and are evident as distinct clusters. These clusters change in size, density, and position as development proceeds. Most dying cells are neurons, and the others are glia. The second round of cell death occurs from 48 h APF

* Corresponding author. Fax: +81 42 367 5626.
E-mail address: tsujmr@cc.tuat.ac.jp (H. Tsujimura).

0012-1606/$ - see front matter © 2012 Elsevier Inc. All rights reserved.
http://dx.doi.org/10.1016/j.ydbio.2012.11.002

to eclosion; only a few cells die during this second round. The optic lobe cell death is apoptosis (Togane et al., 2012).

Ecdysone is an insect steroid hormone that regulates larval development and metamorphosis. During the first half of metamorphosis, when the first round of cell death takes place, there are three ecdysone pulses—the late-larval pulse, the prepupal pulse, and the pupal pulse (Riddiford, 1993). The late-larval pulse peaks at the onset of metamorphosis and initiates pupariation. The prepupal pulse is a small peak at 10 h APF and is necessary for the prepupal–pupal transition. The pupal pulse is the large surge that peaks about 30 h APF and is responsible for adult development.

Ecdysone is received by a heterodimeric nuclear hormone receptor, EcR/USP (Koelle et al., 1991; Riddiford et al., 2000; Thomas et al., 1993; Yao et al., 1993, 1992). The receptor binds to ecdysone response elements (EcREs) to regulate target gene expression in multiple tissues (Cherbas et al., 1991; Riddihough and Pelham, 1987). The *EcR* gene encodes three isoforms—EcR-A, EcR-B1, and EcR-B2 (Talbot et al., 1993). These isoforms result from alternative splicing, and all share a common DNA binding domain and a common ligand binding domain, but each has a unique A/B domain in their N-terminal. EcR-B1 and EcR-B2 each have activation function (AF1) in the A/B domain; EcR-A lacks AF1 and instead has an inhibitory function in the A/B domain; EcR-B1 and EcR-B2 lack this inhibitory function (Mouillet et al., 2001). EcR-A and EcR-B1 isoforms are expressed in different spatial and temporal patterns, and are suggested to have different functions (Talbot et al., 1993; Truman et al., 1994). In fact, loss of EcR-B1 leads to developmental arrest at the onset of metamorphosis and defects in many developmental events—including a pruning of neurons, tanning of puparium, and replacement of larval with imaginal tissues in the midgut and abdomen (Bender et al., 1997; Lee et al., 2000). In contrast, EcR-A mutants arrest development at mid- and late-pupal stages and have abnormally persistent salivary glands and malformed legs (Davis et al., 2005).

Many researchers have reported that ecdysone-regulated cell death occurs during metamorphosis (reviewed by Yin and Thummel, 2005). In the first half of metamorphosis, ecdysone activates cell death in the larval midgut (Jiang et al., 1997; Lee et al., 2002a), salivary glands (Jiang et al., 1997, 2000; Lee et al., 2002b), and two distinct groups of neurons in the ventral nervous system—vCrz neurons (Choi et al., 2006) and RP2 neurons (Winbush and Weeks, 2011). The vCrz neurons require EcR-B2 for cell death; in contrast, the RP2 neurons require EcR-B (B1 and/or B2). Moreover, there is molecular genetic relationship between ecdysone signals and cell death; specifically, *reaper*, a cell death-inducing factor, and *Dronc*, an initiator caspase, each have an EcRE within their respective promoters (Cakouros et al., 2004; Jiang et al., 2000).

In this study, we analyzed the role of ecdysone signaling in the cell death that occurs during development of the optic lobe; specifically, we focused on the expression and function of EcR-A and EcR-B1. First, we examined expression of each isoform and found that they were expressed in different patterns both in neurons and in glia within the developing optic lobe. We then used isoform-specific mutants to investigate the function of each protein and found that cell death in the prepupal stage occurred in an ecdysone-independent manner and the cell death in the later stages occurred in an ecdysone-dependent manner. Moreover, we found that the ecdysone-dependent cell death required EcR-B1.

Materials and methods

Fly strains

Canton-Special was used as the wild-type strain. We used three GAL4 lines, *M1B repo-GAL4* (Sepp et al., 2001), *C155 elav-GAL4* (Lin and Goodman, 1994) and *NP6099-GAL4* (Hayashi et al., 2002), and three UAS lines, *UAS-GFP.nls14* (Bloomington *Drosophila* Stock Center), *UAS-P35.H* (Bloomington *Drosophila* Stock center) and *UAS-EcR-RNAi*^{104} (Colombani et al., 2005). We used two EcR-A mutants, *EcR*^{112} and *EcR*^{139} (Carney et al., 2004), and two EcR-B1 mutants, *EcR*^{Q50st} and *EcR*^{W53st} (Bender et al., 1997). The constructs used to knockdown EcR and FTZ-F1 were *hs-EcRi-11* and *hs-FFi-24*, respectively (Lam and Thummel, 2000). Flies were reared on a general cornmeal-yeast medium at 25 °C under 12 h/12 h light/dark photoperiod.

Detection of dying cells

A modified version of the TUNEL (terminal deoxynucleotide transferase dUTP nick and labeling) method described by Kimura (1995) was used to detect dying cells. Briefly, brains were excised, washed in PBS, fixed in 4% formaldehyde, washed with PBS containing Triton-X (PBS-Tx), and stored in methanol at −20 °C for at least one night. These brains were then washed with PBS-Tx, treated with Protease K (Wako Pure Chemical Industries, Osaka) for 10 min at room temperature, and fixed again in 4% formaldehyde. The brains were subsequently washed with PBS-Tx, pretreated in terminal deoxynucleotidyl transferase (TdT) buffer, and incubated overnight at 37 °C in TdT reaction solution (Takara Bio, Shiga) with biotin-16-dUTP (Roche Diagnostics, Mannheim). The brains were next washed with PBS-Tx and incubated in ABC reaction solution (Vector Laboratories, Burlingame, CA) for 1 h at room temperature. After washing with PBS-Tx, the brains were stained using a standard brown horseradish peroxidase reaction with 3,3′-diaminobenzidine and hydrogen peroxide. Dying cells appeared dark brown. After the reaction, the brains were washed with distilled water, dehydrated in a series of ethanol solutions of increasing concentrations, cleared with methyl benzoate, and embedded in Canada Balsam:methyl benzoate 3:1 (V:V) on a glass slide. The specimens were inspected with bright-field microscopy (Optiphot, Nikon, Tokyo).

Analysis of the number and distribution of dying cells

We used a light microscope, a × 40 objective lens, and a digital camera (TS-CA series, Sugitoh Co., Ltd., Tokyo) to acquire images of dying cells; we then digitally enlarged these images to × 1000 on a monitor. While we gradually shifted the focus, each signal larger than 0.7 μm in diameter was scored as a dying cell with a dot on a transparent plastic sheet that was affixed to the monitor. We used images from the anterior view to count the number of dying cells. The images were captured digitally with a scanner and the number of dying cells was counted using the particle counter module of the NIH ImageJ software package. For the analysis of spatial distribution of dying cells, we obtained images of 1 μm-thick serial optical sections that were taken from a dorsal view. Optical microscope (BX50, Olympus, Tokyo), a digital camera (DP72, Olympus, Tokyo), and Metamorph software (MDS Analytical Technologies, Sunnyvale) were used for this imaging.

Heat induction of dsRNA

To induce RNAi with EcR and βFTZ-F1 before puparium formation, late third instar larvae were placed into 1.5 ml microcentrifuge tubes, and these tubes were incubated for 30 min in a 37 °C water bath. Then, the larvae were transferred into new culture vials and maintained at 25 °C. The animals that underwent pupariation 12–16 h after the heat-shock were used for the experiments. To induce RNAi with EcR after puparium formation, prepupae were subjected to a heat shock twice. They were placed into 1.5-ml microcentrifuge tubes at 0 h APF, and these tubes

were incubated for 45 min in a 37 °C water bath (the first heat shock). Then the prepupae were reared at 25 °C and subjected to the second heat shock at 6 h APF (45 min, 37 °C). Then they were reared at 25 °C and used for the experiment at 24 h APF.

Immunohistochemistry and confocal microscopy

Pupal brains were dissected from whole animals in PBS and fixed in 4% formaldehyde for 20 min. These samples were then washed with PBS-Tx and incubated in PBS-Tx containing a blocking agent (5% normal goat serum) for 30 min. Samples were then incubated in PBS-Tx containing one or two of the following primary antibodies. The primary antibodies were used at the following dilutions: anti-EcR-A (15G1a, Talbot et al., 1993) (1:20), anti-EcR-B1 (AD4.4, Talbot et al., 1993) (1:10), anti-βGal (40–1a, Sanes, J.R.) (1:20), anti-BrdU (G3G4, George-Weinstein et al., 1993) (1:20), anti-Elav (Rat-Elav-7E8A10, O'Neill et al., 1994) (1:20), anti-Repo (8D12, Alfonso and Jones, 2002) (1:20), anti-DE-cadherin (DCAD2, Oda et al., 1994) (1:20), and anti-deadpan guinea pig (a gift from J. Skeath) (1:500). Samples were washed in PBS-Tx for 1 h and then incubated in PBS-Tx containing 5% normal goat serum for 30 min and finally in PBS-Tx containing secondary antibodies. The following secondary antibodies were used: anti-mouse IgG Texas Red (ROCKLAND, Gilbertsville, PA) (1:500), anti-rat IgG Cy5 (Biological Detection Systems, Pittsburgh) (1:100), anti-guinea pig IgG Texas Red (Vector Laboratories, Burlingame) (1:100). After washing for 1 h with PBS-Tx, the antibody-labeled samples were mounted with 80% glycerol (for fluorescence microscope, MERCK, Darmstadt). All images were obtained with a LSM 710 microscope (Carl Zeiss, Oberkochen); the images were processed with Zen2009 light edition (Carl Zeiss, Oberkochen) and Photoshop (Adobe, San Jose).

Results

The expression patterns of EcR isoforms in the developing optic lobe

Riddiford et al. (2010) and Truman et al. (1994) described the expression patterns of EcR isoforms in the developing optic lobe during metamorphosis. EcR-A and EcR-B1 are expressed in optic lobe neurons until 50 h APF, and EcR-A predominates thereafter. EcR-A is also expressed in subsets of glia (Truman et al., 1994). This description, however, is not detailed enough to address the relationship between EcR expression and cell death, which takes place in a complex pattern. Therefore, we analyzed the expression pattern of EcR-A and EcR-B1 in detail here. In this analysis, *UAS-GFP.nls14/+; repo-GAL4/+* was used to mark glial cells with GFP and distinguish them from the other types of cells — such as neuroepithelial cells, neuroblasts, and neurons — that did not express GFP. The boundaries of subregions in the optic lobe were defined by GFP-labeled glial cytoplasm. In the optic lobe, repo-GAL4 was expressed in all glial cells except those located anterolaterally to the medulla neuropil at 24 h APF (Togane et al., 2012). The patterns of GFP expression at 0, 12, and 36 h APF were the same as that at 24 h APF. At 48 h APF, repo-GAL4 was expressed in all optic lobe glia (data not shown).

The anti-EcR-A and anti-EcR-B1 antibodies were used to detect EcR isoforms. Reactions with mouse anti-BrdU or mouse anti-*β*-Gal and reactions lacking any primary antibody were performed as negative controls. In these control reactions, no staining was observed in the nuclei, although the cytoplasm in individual cells was stained at different intensities. Therefore, for the purposes of this assay any cell with nuclear staining was considered as an EcR-expressing cell. If nuclei had stronger staining than did the cytoplasm, we described the expression as "strong". If staining in the nucleus was weaker than that in the cytoplasm, we described the expression as "weak". If levels of staining in nucleus and the cytoplasm were similar, we described the expression as "moderate" or just as "expressed".

The lamina, medulla, lobula plate cortices, and the region of T2/T3/C neurons (T/C region) were identified based on our previous work (Togane et al., 2012). We have performed a study on the locations of the OOA and IOA including neuroblasts and neuroepithelial cells at each developmental stage and are preparing a paper on this subject. In the following description, locations of the OOA and IOA were identified by relative positions among substructures based on the study (Fig. 1A, B).

For both EcR-A and EcR-B1, we found that expression patterns often differed between the areas where neurons were ensheathed by glial cytoplasm (ensheathed domains) and the areas where neurons were not yet ensheathed (pre-ensheathed domains). Therefore, we will describe EcR expression using the terms "ensheathed domain" and "pre-ensheathed domain" henceforth. First, we describe the distribution of the two domains in the developing optic lobe cortices.

Lamina neurons are produced by the OOA and added to the developing lamina cortex at the anterior side (Fischbach and Hiesinger, 2008; Meinertzhagen and Hanson, 1993). Then, newly

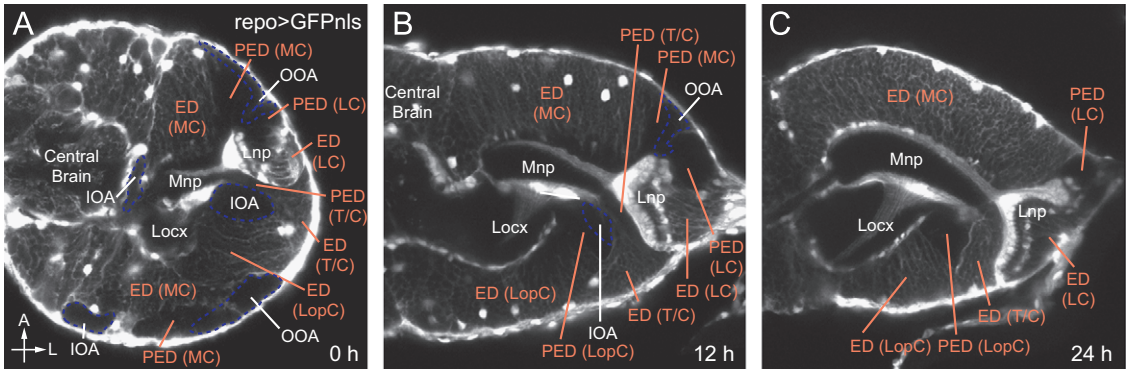

Fig. 1. Distribution of ensheathed domain and pre-ensheathed domain in the developing optic lobe in *UAS-GFP.nls14/+*; *repo-GAL4/+*. Glial cell bodies and cytoplasm were GFP-labeled. All images are obtained from single sections from the dorsal view. (A) At 0 h APF, pre-ensheathed domains were located in the anterior side of the lamina cortex, the lateral side of the medulla cortex and deep inside the T/C region. The lobula plate cortex was entirely occupied by the ensheathed domain. (B) At 12 h APF, pre-ensheathed domains were located in the anterior side of the lamina cortex, at the lateral edge of the medulla cortex, deep inside the T/C region and the anterolateral side of the lobula plate cortex. (C) At 24 h APF, pre-ensheathed domains were located at the anterior edge of the lamina cortex and in the anterolateral side of the lobula plate cortex. In the medulla cortex and the T/C region, ensheathed domain stretched entirely. *Abbreviations*: ED, ensheathed domain; PED, pre-ensheathed domain; LC, lamina cortex; MC, medulla cortex; LopC, lobula plate cortex; T/C, T2/T3/C neurons; Lnp, lamina neuropil; Mnp, medulla neuropi; Locx, lobula complex; OOA, outer optic anlagen; IOA, inner optic anlagen; A, anterior; L, lateral.

born lamina neurons are located at the anterior side of the lamina cortex and older neurons at the posterior side. Neurons align in order from older to younger neurons to form columnar structures (Meinertzhagen and Hanson, 1993). In this study, we found the proximal satellite glia (psg) (reviewed by Edwards and Meinertzhagen, 2010; Edwards et al., 2012) were involved in the formation of lamina columns. The psg near the surface of the lamina cortex migrated inwards to separate each column at the last phase of the formation of columnar structures. These migrations proceeded in a posterior to anterior order in the cortex. As a result, an ensheathed domain was located in the posterior side of the lamina cortex, and a pre-ensheathed domain occupied a region between the lamina furrow and the ensheathed domain at 0–24 h APF (Fig. 1A–C). Neurons were distributed randomly in the pre-ensheathed domain, while they aligned to form columnar structures in the ensheathed domain. The ensheathed domain reached to the anterior edge of the cortex by 36 h APF. Neurons in the ensheathed domain were elav-positive; this finding indicated they were differentiated lamina neurons (data not shown).

Medulla neurons are derived from neuroblasts in the medial side of the OOA (Meinertzhagen and Hanson, 1993; Fischbach and Hiesinger, 2008). Thus, older neurons are located in the medial side of the medulla cortex, and newly born neurons are located in the lateral side of the cortex. At 0–12 h APF, we observed a pre-ensheathed domain on the lateral side of the medulla cortex beneath the OOA and just medial to the lamina furrow. The other region of the cortex was an ensheathed domain (Fig. 1A, B). The pre-ensheathed domain was gone by 24 h APF, and the entire cortex was occupied by an ensheathed domain (Fig. 1C).

T/C and lobula plate neurons are derived from the IOA, which is located deep within the optic lobe near the anterolateral end of the lobula plate neuropil. In the T/C region between 0 and 12 h APF, a pre-ensheathed domain was located in a small region between the lamina neuropil and the IOA (Fig. 1A, B); the other region in this area was an ensheathed domain. The pre-ensheathed domain was gone by 24 h APF (Fig. 1C).

In the lobula plate cortex, all neurons throughout this cortex were ensheathed, and there was no pre-ensheathed domain at 0 and 6 h APF (Fig. 1A). However, there was a small pre-ensheathed region at 12 and 24 h APF (Fig. 1B, C); this small region was where neuroblasts of the IOA had been located at the previous stage. The other region in this cortex was an ensheathed domain. The pre-ensheathed domain was gone by 36 h APF.

In the following two sections, we will describe an overall EcR-B1 expression in neurons (Fig. 2) and glia (Fig. 3). Fig. 4 shows expression maps of EcR-B1 based on the results from this analysis. More detailed description of EcR-B1 expression at each stage is summarized in supplemental Tables 1 and 3. Description of EcR-A expression is presented in supplemental Figs. 1–3, and supplemental Tables 2 and 3, since EcR-A was not important for the optic lobe cell death as shown in later sections.

EcR-B1 expression in the optic lobe neurons, the OOA and IOA

At 0 h APF, EcR-B1 was not expressed in any region of the optic lobe (Figs. 2A and 4A) except for three cells, the optic lobe pioneers (OLPs) (Tix et al., 1989), which were located between the lamina cortex and the T/C region (arrows in Fig. 2I).

At 6 h APF, the expression of EcR-B1 in the OLPs was lost and no expression was evident within entire optic lobe (Fig. 2B).

During 9–48 h APF, EcR-B1 expression was observed and its expression pattern was different among regions. Then, we describe the pattern separately below. We skip to describe the expression pattern at 9 h APF as it was almost the same at 12 h APF (Fig. 2C, D; Table S1).

Lamina cortex

At 12 h APF, EcR-B1 was weakly expressed in the pre-ensheathed domain behind the lamina furrow (Figs. 2D, J, J′ and 4B). In the ensheathed domain, EcR-B1 was strongly expressed. EcR-B1 expression at 24 h APF was similar to that at 12 h APF, though the pre-ensheathed domain shrank to become a small region adjacent to the lamina furrow and the ensheathed domain expanded in the anterior direction (Figs. 2E, N, N′ and 4C). At 36 h APF, as the ensheathed domain reached the anterior edge of the lamina cortex, EcR-B1 was expressed across the cortex more strongly than at 24 h APF (Fig. 2F). At 48 h APF, the expression of EcR-B1 became weaker in some neurons, but it remained strong in the other neurons (Fig. 2G). By 60 h APF, EcR-B1 expression disappeared in any cells (Fig. 2H).

Medulla cortex and T/C region

At 12 h APF, EcR-B1 was not expressed in the pre-ensheathed domain in both regions, but it was expressed in the ensheathed domain (Figs. 2D, K, K′, L, L′and 4B). At 24 h APF, the ensheathed domain expanded entirely in each region, and EcR-B1 was strongly expressed almost across the regions (Figs. 2E and 4C). At 36 h APF, EcR-B1 expression became stronger (Fig. 2F). At 48 h APF, in the medulla cortex, the expression of EcR-B1 became weaker in some neurons, but remained strong in the other neurons (Fig. 2G). In the T/C region, EcR-B1 expression was uniformly strong (Fig. 2G). By 60 h APF, EcR-B1 expression disappeared in both regions (Fig. 2H, S).

Fig. 2. EcR-B1 expression in the optic lobe neurons, OOA and IOA in *UAS-GFP.nls14/+*; *repo-GAL4/+*. Optic lobes were stained with anti-EcR-B1 antibody. All images were obtained from single sections from the dorsal view except (M) and (P), which were obtained from the posterior view. (A–H) Overall view of the optic lobe at (A) 0 h, (B) 6 h, (C) 9 h, (D) 12 h, (E) 24 h, (F) 36 h, (G) 48 h and (H) 60 h APF. (C) At 9 h APF, EcR-B1 expression was stronger in the lateral half of the medulla cortex (filled-arrow) than in the medial half (outlined-arrow). (C–G) At 9–48 h APF, EcR-B1 was not expressed in regions deep in the medial side of the medulla cortex (filled-arrowheads). (E) At 24 h APF, EcR-B1 was not expressed in a small number of cells deep inside the lobula plate cortex (arrow). (F, G) Arrows indicate neurons between medulla and lobula plate neuropils. Outlined-arrowheads indicate regions of highest level of expression in the lobula plate cortex at 36 and 48 h APF, respectively. (H) EcR-B1 was not expressed throughout the optic lobe at 60 h APF. Although signal was strong at the lamina region at this stage, it was due to the staining in the cytoplasm but not in the nuclei, indicating EcR-B1 was not expressed there. (I) Image from a section more ventral than I-square in (A). Arrows indicate the optic lobe pioneers. (J, J′) The white square region in (D). In the lamina cortex, cells did not express EcR-B1 at 12 h APF at the lateral side of the lamina furrow (arrows) and at the boundary between the pre-ensheathed and ensheathed domains (filled-arrowheads). Outlined-arrowheads indicate L5 neurons adjacent to the larval epithelial glia in the pre-ensheathed domain. They moderately expressed EcR-B1. (K, K′) The dotted square region in (D). Arrows indicate cells in the OOA which weakly expressed EcR-B1. (L, L′) The red square region in (D). (M) Image obtained from the posterior view of the optic lobe at 12 h APF. In the PMR (encircled by dotted line), EcR-B1 was not expressed in most neurons located in its dorsal side (arrow), but was weakly expressed in the ventral side (arrowhead). (N, N′) The square region in (E). Arrows indicate cells which did not express EcR-B1 at the boundary between the pre-ensheathed and ensheathed domains in the lamina cortex. (O) Magnified image obtained from a section more dorsal than (E), focusing on the PMR at 24 h APF. (P) An image obtained from the posterior view of the optic lobe at the level of the red line in (E). EcR-B1 was weakly expressed in the PMR, except a small area centrally located in dorsoventral axis (arrow). (Q) Image obtained from a section more dorsal than (F), focusing on the PMR at 36 h APF. (R) Magnification of (Q). Arrows indicate large cells which did not express EcR-B1 inside the PMR. (S) Magnification of the medulla cortex at 60 h APF. *Abbreviations*: ED, ensheathed domain; PED, pre-ensheathed domain; LC, lamina cortex; MC, medulla cortex; LopC, lobula plate cortex; T/C, T2/T3/C neurons; PMR, posteromedial region; OOA, outer optic anlagen; IOA, inner optic anlagen; Mnp, medulla neuropi; Locx, lobula complex; Lf, lamina furrow; CB, central brain; lveg, larval epithelial glia; A, anterior; P, posterior; L, lateral; M, medial; D, dorsal; V, ventral. Scalebars=20 μm.

Lobula plate cortex

At 12 and 24 h APF, EcR-B1 was expressed almost throughout the cortex in a gradient; the level was high in the posteromedial side and low in the anterolateral side (Figs. 2D, E, L, L′ and 4B, C). At 36 h APF, EcR-B1 was expressed strongly across the cortex (Fig. 2F). The gradient that had been observed at 24 h APF was gone, and the strongest expression was observed near the posterior surface of the cortex (outlined-arrowhead in Fig. 2F). At 48 h APF, EcR-B1 was expressed strongly in a gradient with the highest level at the lateral side (outlined-arrowhead in Figs. 2G and 4D). By 60 h APF, EcR-B1 expression disappeared (Fig. 2H).

PMR

Since medial region of the lobula plate cortex had a different overall pattern of EcR-B1 expression than did any other part of the cortex, we named this region the posteromedial region (PMR)

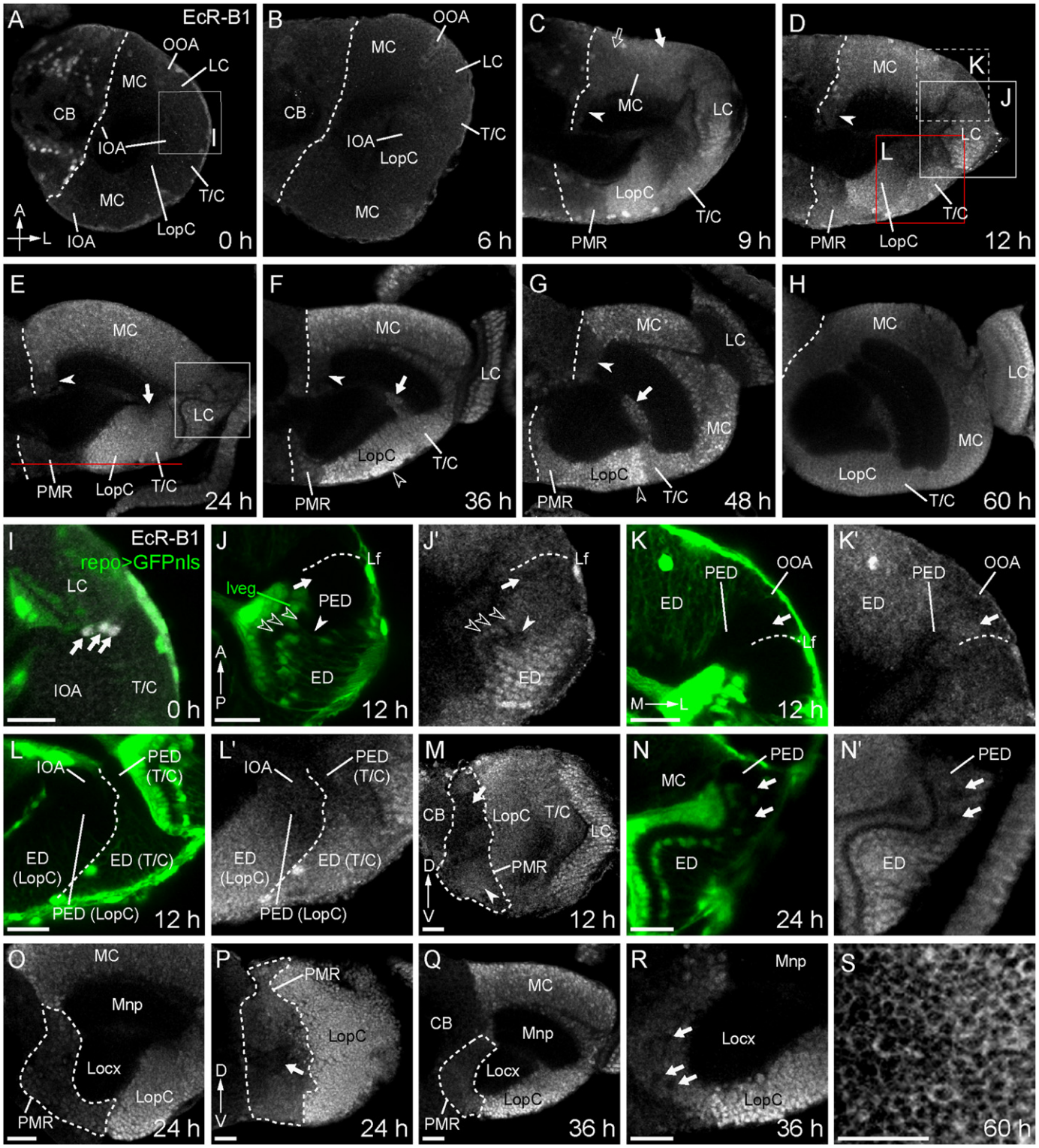

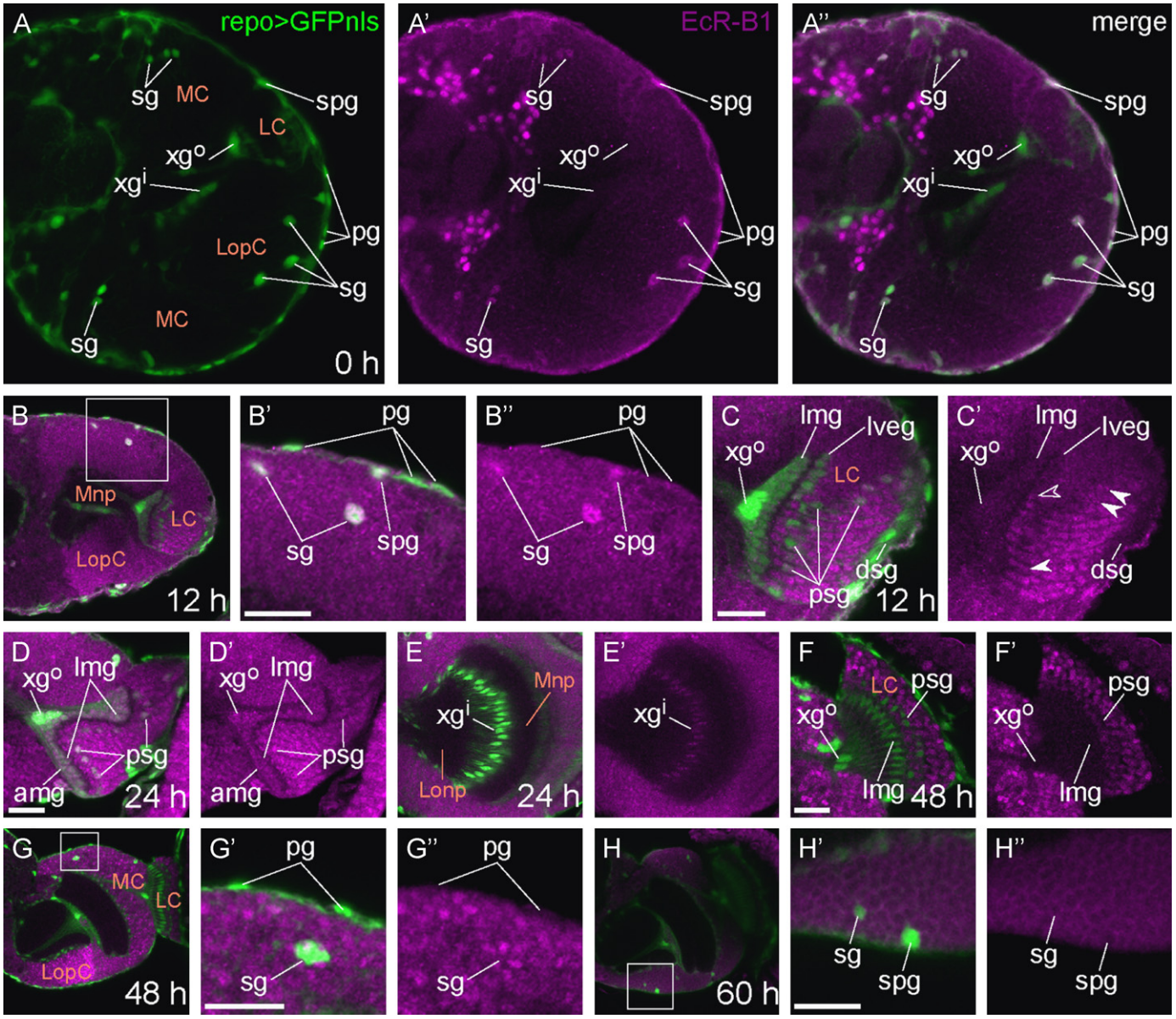

Fig. 3. EcR-B1 expression in the optic lobe glia in *UAS-GFP.nls14/+; repo-GAL4/+*. (A–H″) All images were obtained from single sections from the dorsal view except (E) and (E′), which were obtained from the anterior view. Optic lobes were stained with anti-EcR-B1 antibody. (A–A″) At 0 h APF, EcR-B1 was expressed in the pg, spg and sg. (B–B″) At 12 h APF, EcR-B1 was expressed in the pg, spg and sg. B′ and B″ are the square region in (B). (C, C′) At 12 h APF, EcR-B1 was expressed in some psg (filled-arrowheads) and in some lveg (outlined-arrowhead). (D, D′) At 24 h APF, EcR-B1 was strongly expressed in the psg and weakly in the lmg, amg and xg^o. (E, E′) At 24 h APF, EcR-B1 was weakly expressed in the xg^i. (F, F′) At 48 h APF, EcR-B1 expression in the psg, lmg, amg and xg^o disappeared. The amg was on different focal planes of the sample and not seen. (G–G″) At 48 h APF EcR-B1 was weakly expressed in the sg, but not in the pg. G′ and G″ are the square region in (G). (H–H″) At 60 h APF, EcR-B1 expression disappeared in the sg and spg. H′ and H″ are the square region in H. *Abbreviations*: psg, proximal satellite glia; dsg, distal satellite glia; lveg, larval epithelial glia; lmg, larval marginal glia; amg, adult marginal glia; xg^o, outer chiasmal glia; xg^i, inner chiasmal glia; sg, satellite glia; pg, perineurial glia; spg, subperineurial glia; LC, lamina cortex; MC, medulla cortex; LopC, lobula plate cortex; Mnp, medulla neuropi; Lonp, lobula neuropil. Scalebars=20 μm.

(Fig. 2C–G), and here describe EcR-B1 expression in this region separately from the lobula plate cortex. At 12 h APF, EcR-B1 was not expressed in most neurons located on the dorsal side of PMR (arrow in Fig. 2 M), but it was weakly expressed on the ventral side (arrowhead in Fig. 2M) of this region. At 24 h APF, EcR-B1 was weakly expressed in most cells (Fig. 2O, P). At 36 and 48 h APF, EcR-B1 expression was stronger than that at 24 h APF (Fig. 2F, G, Q, R and 4D). By 60 h APF, EcR-B1 expression disappeared (Fig. 2H).

OOA and IOA

At 12 h APF, in the OOA, weak expression was observed only in some cells on the medial side of the lamina furrow (arrows in Figs. 2K, K′ and 4B). EcR-B1 was not expressed in the IOA (Figs. 2L, L′ and 4B).

EcR-B1 expression in the optic lobe glia

The types of glia were basically identified based on Edwards and Meinertzhagen (2010) and Edwards et al. (2012). However, we found in a related project that the epithelial glia (eg) and the marginal glia (mg) in the lamina cortex at the larval stage did not develop into the adult eg and mg. To avoid confusion, we refer to larval eg and mg as lveg and lmg, respectively, and adult mg as amg.

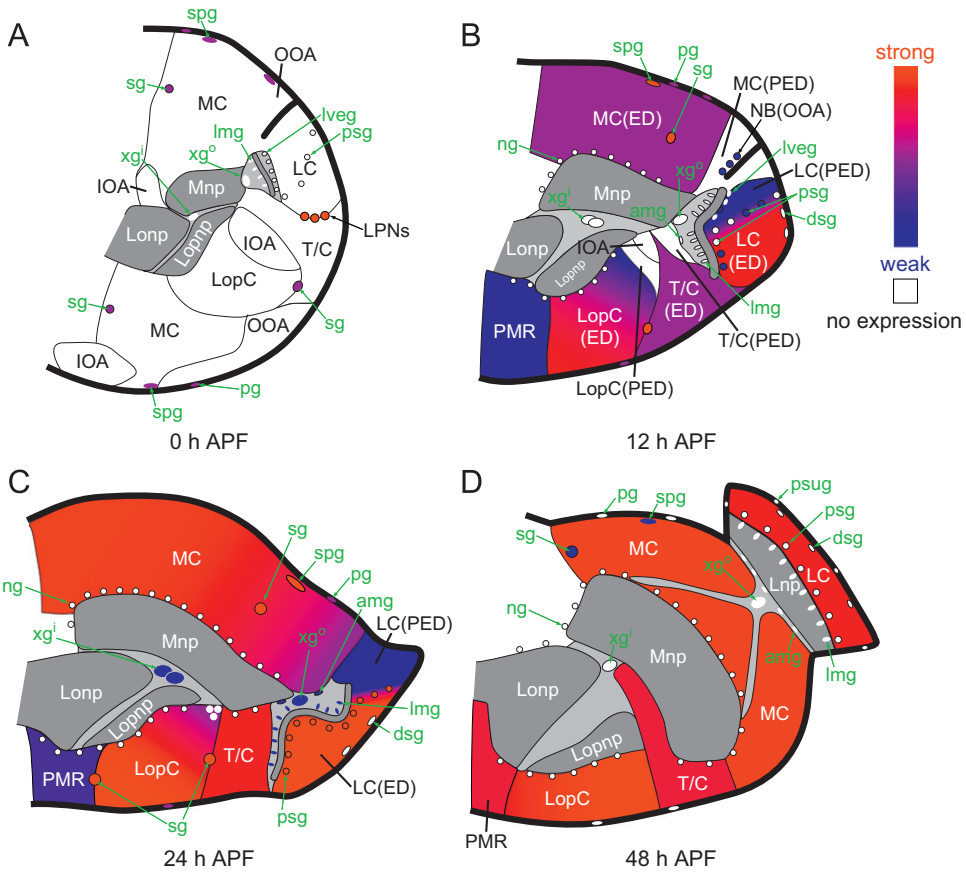

Fig. 4. Expression maps of EcR-B1. (A–D) Schematic diagrams of a single horizontal section midway in the dorsoventral axis at (A) 0 h, (B) 12 h, (C) 24 h and (D) 48 h APF. Red color indicates a strong expression and blue color indicates a weak expression. No color (white) indicates no expression. Dark gray, neuropils; Light gray, cytoplasm of glia. *Abbreviations*: LC, lamina cortex; MC, medulla cortex; LopC, lobula plate cortex; T/C, region of T2/T3/C neurons; PMR, posteromedial region; Lnp, lamina neuropil; Mnp, medulla neuropi; Lonp, lobula neuropil; Lopnp, lobula plate neuropil; psg, proximal satellite glia; dsg, distal satellite glia; lveg, larval epithelial glia; lmg, larval marginal glia; amg, adult marginal glia; psug, pseudocartridge glia; xg^o, outer chiasmal glia; xg^i, inner chiasmal glia; sg, satellite glia; ng, neuropil glia; pg, perineurial glia; spg, subperineurial glia.

EcR-B1 expression varied among types of glia (Table S3): each type of glia had its specific expression pattern. For brevity of description, we classified the optic lobe glia into four groups based on EcR-B1 expression pattern.

First, in two subtypes of surface glia, the perineurial glia (pg) and the subperineurial glia (spg), EcR-B1 was expressed at 0 h APF (Figs. 3A–A″ and 4A). EcR-B1 was also expressed in the satellite glia (sg) in the medulla and lobula plate cortex and T/C region (Figs. 3A–A″ and 4A). Although EcR-B1 expression in these glia was gone at 6 h APF, it was evident again at 12 h APF (Figs. 3B–B″ and 4B). Then, EcR-B1 expression was gone in the pg at 48 h APF (Fig. 3G–G″) and in spg and sg at 60 h APF (Fig. 3H–H″).

Second, in the psg and lveg, EcR-B1 was expressed in some of them at 12 h APF (filled-arrowheads and outlined-arrowhead in Figs. 3C, C′ respectively, 4B). At 24 h APF, EcR-B1 was strongly expressed in the psg and lveg (Figs. 3D, D′ and 4C). The lveg was not identifiable themselves after 36 h APF. Expression in the psg was gone by 48 h APF (Fig. 3F, F′).

Third, in the lmg, amg and outer chiasmal glia (xg^o) in the lamina region (Figs. 3D, D′, 4C) and inner chiasmal glia (xg^i) between the medulla and lobula neuropil (Figs. 3E, E′, 4C), EcR-B1 was weakly expressed at 24 h APF. EcR-B1 expression was gone in the xg^i at 36 h APF and in the lmg, amg, xg^o at 48 h APF (Fig. 3F, F′).

Finally, in the distal satellite glia (dsg) (Fig. 3C, C″), pseudocartridge glia (psug), carpet glia (cg) and neuropil glia (ng), EcR-B1 was not expressed at any stages (Fig. 4A–D, Table S3).

The optic lobe cell death occurs in EcR-B1 dependent and independent ways

In the optic lobe, EcR-A and EcR-B1 were expressed in different patterns. This difference indicated that these isoforms had different roles in the optic lobe development. Therefore, we examined the roles of EcR-A and EcR-B1 in the optic lobe cell death using isoform-specific mutants.

EcR^{Q50st} and EcR^{W53st} are EcR-B1 mutant alleles; each carries a stop codon within the EcR-B1-specific exon 2 (Bender et al., 1997). The average number of dying cells in the optic lobe at 0 h APF in the trans-heterozygote (EcR^{Q50st}/EcR^{W53st}) was 509.5, which is nearly the same as 545.8, the number in the wild-type (Fig. 5A). The average number of dying cells in the mutant at 12 h APF (690.6) was smaller, but not significantly different from that in the wild-type (854.4). In most mutant samples, the number of dying cells was about 800 at this stage, nearly the same as that in the wild type (4 of the 5 optic lobes, 4/5), while it was much smaller (about 300) in 1 of the 5 mutant samples. At 24 h APF, the number of dying cells in the mutant decreased and was 67% smaller than that in the wild-type (363.8 (mutant) versus 1112.6 (wild type); $P<0.01$, Mann–Whitney U-test). At 36 h APF, the number in the mutant decreased further to 300, which was 56% smaller than that in the 678.2 in the wild-type ($P<0.01$). The number of dying cells in the mutant remained constant (about 300) from 48 to 72 h APF, during this period only a few cell deaths occur in the wild type. Taken together, these results indicated that

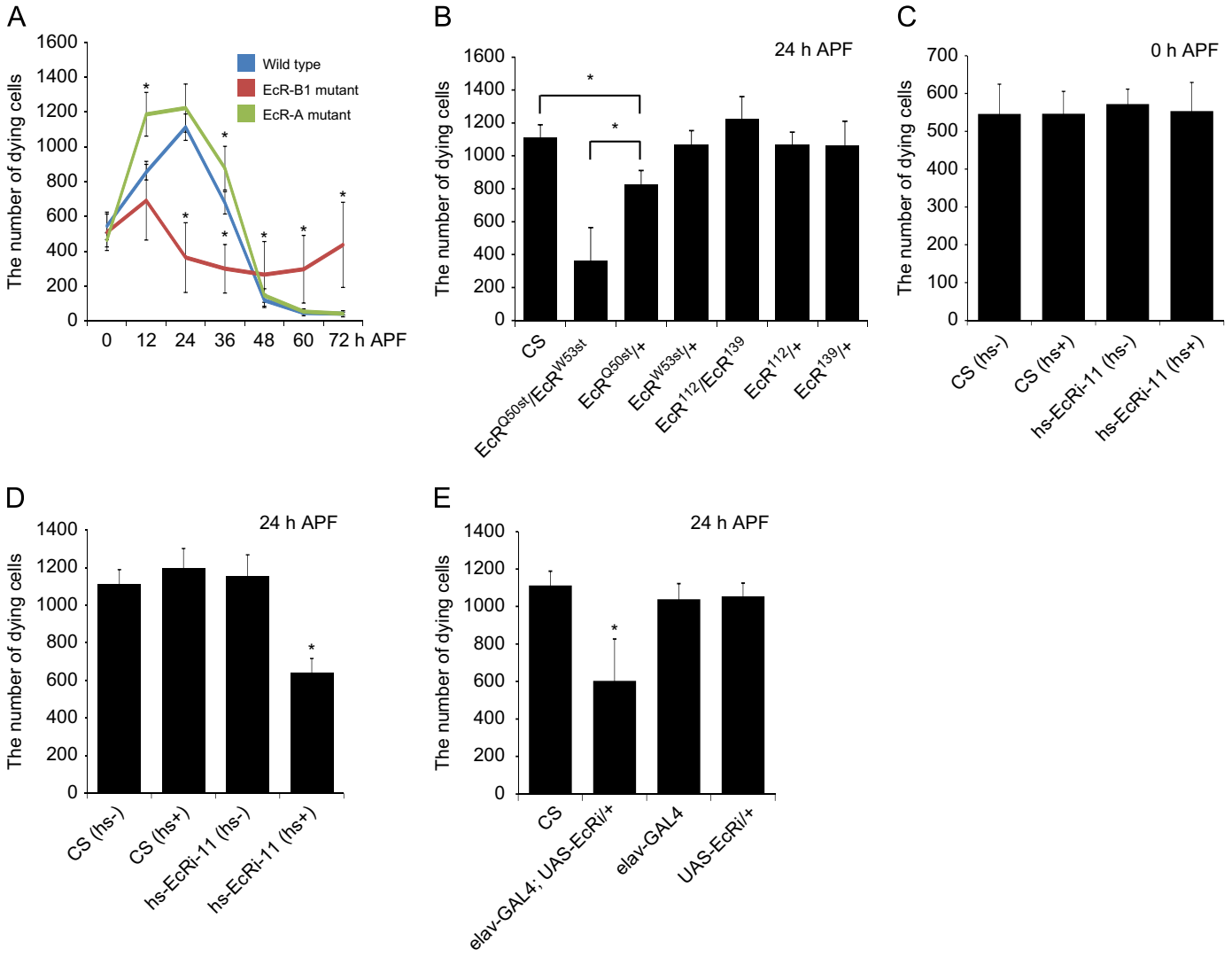

Fig. 5. EcR-B1 was required for the optic lobe cell death at 24 and 36 h APF, but any isoforms was not required at 0 h APF. (A) Temporal change in the number of dying cells in the wild type, EcR-A mutant (EcR^{112}/EcR^{139}) and EcR-B1 mutant (EcR^{Q50st}/EcR^{W53st}). Dying cells were detected by TUNEL staining. $n=10$ for 24 h APF. $n=5$ for the other time points. (B) The number of dying cells at 24 h APF in heterozygotes of the mutant alleles, $EcR^{112}/+$, $EcR^{139}/+$, $EcR^{Q50st}/+$ *and* $EcR^{W53st}/+$, $n=10$. (C) Effects of a heat-shock inducible EcR RNAi on the number of dying cells in the optic lobe at 0 h APF. A heat shock (hs+) was given at 12–16 h BPF in 37 °C water bath for 30 min, $n=5$. (D) Effects of a heat-shock inducible EcR RNAi on the number of dying cells at 24 h APF. Heat shock (hs+) was given at 0 and 6 h APF in 37 °C water bath for 45 min each, $n=5$. (E) Effect of elav > EcR RNAi on the number of dying cells at 24 h APF, $n=10$. Error bars: standard deviation. Asterisks: significant difference ($^*p<0.01$ Mann–Whitney *U*-test).

EcR-B1 was not required for cell death at 0 h APF, but was required between 24 and 36 h APF.

The temporal pattern of the number of dying cells in the optic lobe of EcR-A mutants was different from that of EcR-B1 mutants. EcR^{112} and EcR^{139} are EcR-A mutant alleles that carrying deficiencies of the EcR-A transcription start site and the EcR-A specific exon, respectively (Carney et al., 2004). The average number of dying cells in the trans-heterozygote (EcR^{112}/EcR^{139}) at 0 h APF was 466, which was not significantly different from the 545.8 in the wild-type (Fig. 5A). At 12 h APF, however, the average number of dying cells in the mutant increased dramatically to 1186.4, which was 39% and significantly larger than the 854.4 observed in the wild-type ($P<0.01$). At 24 h APF, the average number of dying cells in the mutant was 1222.2, which was nearly the same as that in the wild-type. The average number of dying cells in the mutant decreased to 146 by 48 h APF, and a few dying cells were observed after 48 h APF, as was also the case in the wild-type. These results suggest that EcR-A was not involved in the optic lobe cell death, although it may have inhibited the cell death at 12 h APF.

At 24 h APF, the average number of dying cells was determined for control samples from heterozygous animals ($EcR^{Q50st}/+$, $EcR^{W53st}/+$, $EcR^{112}/+$, and $EcR^{139}/+$; Fig. 5B). The averages for these heterozygotes were similar to that for the wild-type animals, except that the average for the $EcR^{Q50st}/+$ was 826.3, which was 26% less than that for the wild-type (Fig. 5B). Nevertheless, the average for the EcR^{Q50st}/EcR^{W53st} was still much smaller than that for the $EcR^{Q50st}/+$ ($P<0.01$).

At 0 h APF, the average number of dying cells for the EcR-A or EcR-B1 mutants was not significantly different from that for wild-type animals. This indicated that both isoforms were not required for programmed cell death in the optic lobe cell at this stage. To address whether EcR-B2 was required for the cell death at this stage, we induced RNAi before puparium formation via *hs-EcRi-11* construct (Lam and Thummel, 2000) to knockdown all EcR isoforms; we determined the average number of dying cells in the optic lobe from knockdown animals. The *hs-EcRi-11* construct encodes a dsRNA that is under the control of a heat shock promoter and that targets a coding region common to all EcR

isoforms. When *hs-EcRi-11* homozygous larvae were subjected to heat shock at 37 °C, 12–16 h before puparium formation (BPF), the animals entered a stationary phase, but their bodies did not shorten or form the characteristic shape of prepupa as reported by Lam and Thummel (2000). The average number of dying cells for these heat-shocked animals at the stationary phase was not significantly different from that for the wild-type at 0 h APF (Fig. 5C). This finding indicates that EcR-B2 was also not required for the cell death at 0 h APF.

EcR-B1 was required cell death in the optic lobe between 24 and 36 h APF. This finding raised a question whether the reduction of the number of dying cells was due to the loss of EcR-B1 at prepupal and pupal stages or at earlier developmental stages. To address this question, we induced RNAi specifically after puparium formation. When *hs-EcRi-11* homozygous prepupae were subjected to heat shock (37 °C, 0 and 6 h APF for 45 min each), the average number of dying cells was 638.6 at 24 h APF, which was much smaller than those in controls (Fig. 5D). This result indicates that prepupal and pupal EcR-B1 is required for the optic lobe cell death. We also histologically checked optic lobe development in EcR-B1 mutant at 0, 6 and 12 h APF. There was almost no difference in the distribution of neuroepithelial cells, neuroblasts, neurons and glia between the EcR-B1 mutants and wild type animals at these stages (data not shown), supporting the above idea.

Most clusters of dying cells were lost in EcR-B1 mutant after 24 h APF

Dying cells are not uniformly distributed throughout the optic lobe, but instead appear in several stereotypic patterned clusters in each cortex (Togane et al., 2012). These clusters change in size, density, and position during optic lobe development. This finding indicates that each cluster is governed by a distinct regulatory mechanism. Therefore, we examined the distribution of dying cells in EcR-B1 and EcR-A mutants. Table 1 summarizes the data presented in this section.

We described the distribution of dying cells in optic lobes from wild-type animals in the previous paper (Togane et al., 2012). Based upon our current re-examination, we corrected the names of some clusters in this study and named some new additional clusters. Therefore, we will first describe the correction and the additional clusters in the wild type.

At 12 h APF, we observed a cluster of many dying cells at the ventromedial position in the PMR; this cluster was newly identified and named PMD (posteromedial dying cells) (Fig. 6C).

At 24 h APF, we previously reported that MALD was located on the lateral side of the medulla cortex at this stage. However, based upon the current re-examination, we concluded that this cluster was different from MALD that we had observed at 12 h APF and that dying cells of this cluster newly emerged at this stage; therefore, we renamed this cluster LUD (lamina underlying dying cells) (Fig. 6D, E). This LUD cluster was located just medial to the lamina neuropil at a region where lamina axons extended toward the medulla neuropil and cytoplasm of glia enwrapped the axons. This cluster was lost when p35, a baculovirus-derived cell death inhibitor, was expressed in glia under the control of *repo-GAL4,* but not when p35 was expressed with *elav-GAL4*; these finding demonstrated that dying cells in the LUD cluster were glia.

At 36 h APF, there were many dying cells in the medulla cortex in a position just posterior to the medulla neuropil and we named the dying cells MPLD (medulla posterolateral dying cells) (Fig. 6F). We also observed a cluster of dying cells in the medulla cortex along the boundary with the lamina region; we named this cluster the medulla-lamina boundary dying cells (MLBD) (Fig. 6F). Dying cells in both clusters were neurons (data not shown).

Next, we describe the distribution of dying cells in the EcR-B1 mutant. Because the structure of optic lobes in EcR-B1 mutants after 24 h APF was similar to that in wild-type animals at 12 h APF, we identified clusters of dying cells in the mutants based on the relative position of the substructures in the samples from mutant animals after 24 h APF and those from wild-type animals at 12h APF.

At 0 h APF, there was no difference between the mutant and the wild type in the distribution of dying cells in the optic lobes (Fig. 6A, I).

However, some differences between mutant and wild-type samples were evident at 12 h APF. In most mutant samples (8/10), the LAD, LPD, and MALD clusters and dying cells in T/C region were evident, but the PMD cluster was not (Fig. 6B, C, J). Many dying cells were evident throughout the medulla cortex, but we could not readily classify them into any defined cluster because the regions between the MCLD and MCMD clusters and between the MCMD and MAMD clusters that would have had no dying cells in wild-type samples were absent. In a few cases (2/10), the

Table 1
Distribution of dying cell clusters in the wild type, EcR-B1 mutant and EcR-A mutant.

	0 h APF	12 h APF	24 h APF	36 h APF	48 h APF	72 h APF
Wild type	LAD, MALD, MCD, MAMD, PMCD, T/C (Fig. 6A)	LAD, LPD, MALD, MCLD, MAMD, MCMD, T/C, PMD (Fig. 6B, C)	LAD, LPD, LUD, MCLD, MCMD, T/C (Fig. 6D, E)	LUD, MCMD, MLBD, MPLD, LopD (Fig. 6F)	MPLD (Fig. 6G)	no cluster (Fig. 6H)
EcR-B1mutant	LAD, MALD, MCD, MAMD, PMCD, T/C (10/10) (Fig. 6I)	LAD, LPD, MALD, T/C (8/10)[a] (Fig. 6J, K)	no cluster (9/10) MMC (9/10)[b] (Fig. 6L)	no cluster (10/10) MMC (10/10)[b] (Fig. 6M)	no cluster (7/10) MMC (9/10) (Fig. 6N)	no cluster (6/10) (4/10)[c] MMC (10/10) (Fig. 6O, P)
EcR-A mutant	LAD, MALD, MCD, MAMD, PMCD, T/C (10/10) (Fig. 6Q)	LAD, LPD, MALD, MCLD, MAMD, MCMD, T/C, PMD (10/10) (Fig. 6R)	LAD, LPD, LUD, MCLD, MCMD, T/C (10/10) MLopD (8/10) (Fig. 6S)	no data	MPLD (10/10) (Fig. 6T)	no data

(n/10): number of samples of total 10 samples.
Abbreviations: LAD, lamina anterior dying cells; LPD, lamina posterior dying cells; LUD, lamina underlying dying cells; MALD, medulla anterolateral dying cells; MAMD, medulla anteromedial dying cells; MCD, medulla cortex dying cells; MCLD, medulla cortex lateral dying cells; MCMD, medulla cortex medial dying cells; MLBD, medulla-lamina boundary dying cells; MPLD, medulla posterolateral dying cells; PMCD, posterior medulla cortex dying cells; PMD, posteromedial dying cells; T/C, dying cells in the T/C region; LopD, dying cells in the lobula plate cortex; MMC, abnormal dying cells in the medial side of the medulla cortex; MLopD, abnormal dying cells in the medial side of the lobula plate cortex.

[a] Many dying cells were evident throughout the medulla cortex but we could not classify them into MCLD, MCMD or MAMD.
[b] We could not determine if there was MCMD or not because the region of MCMD and MMC overlapped.
[c] 4 out of 10 samples, many dying cells were observed in the anterior side of the lamina cortex, lateral side of medulla cortex and T/C region.

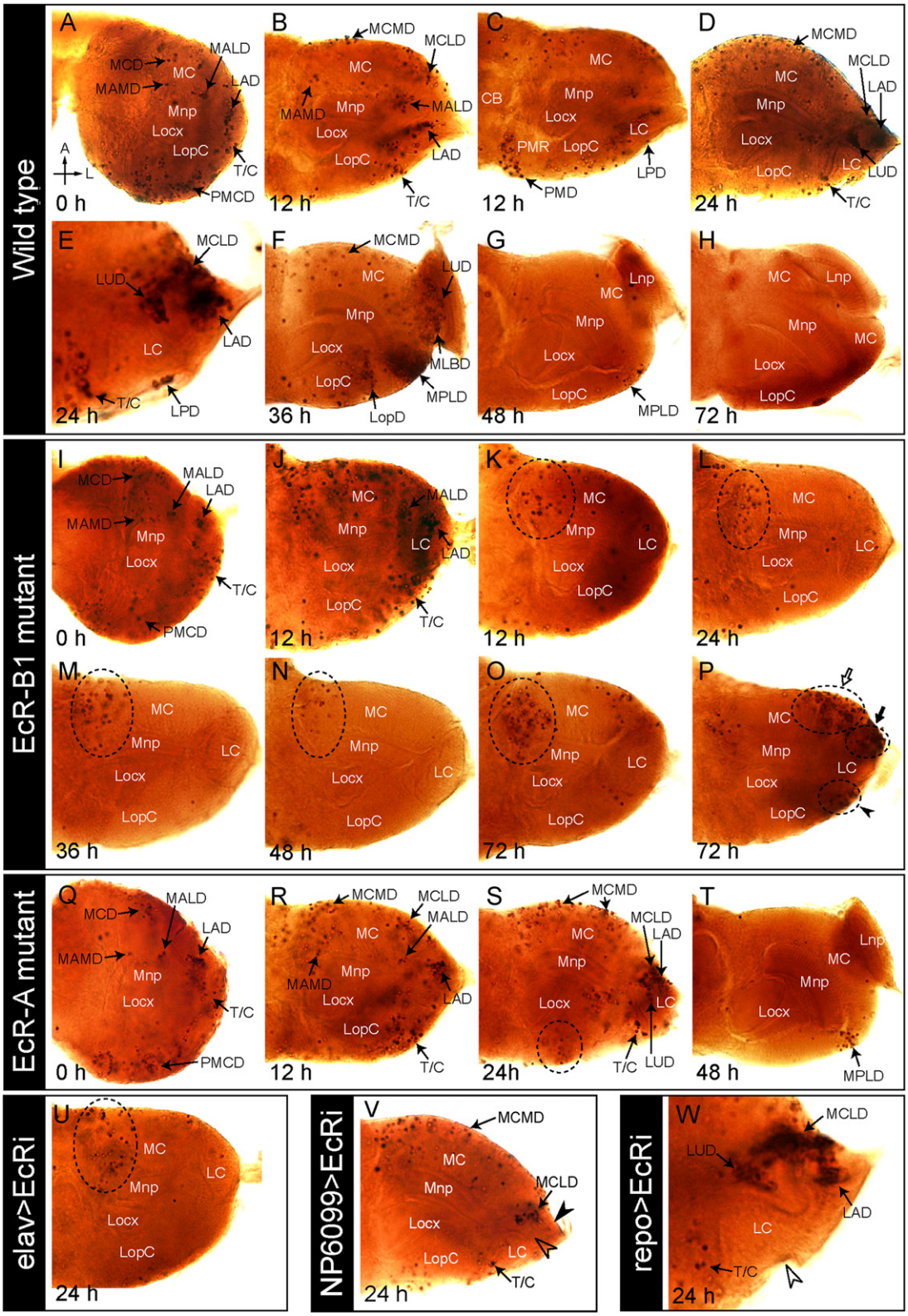

Fig. 6. Most clusters of dying cells were lost in the EcR-B1 mutant after 24 h APF. All images were obtained from optical sections of the optic lobes from the dorsal view. Dying cells were detected by TUNEL staining. LPD at 12 and 24 h APF was on different focal planes of the samples and not seen in B, D, J, R, S and V. (A–H) Distribution of dying cells at different developmental stages in the wild type, CS. (E) Magnification of the lamina region at 24 h APF. (I–P) Distribution of dying cells in the EcR-B1 mutant, EcR^{Q50st}/EcR^{W53st}. (J, K) At 12 h APF, there were many clusters of dying cells in most samples (J), but the clusters were absent in a few samples (K). (P) In some samples at 72 h APF, many abnormal dying cells were observed in the anterior region of the lamina cortex (filled-arrow), the medial side of the medulla cortex (outlined arrow) and the T/C region (arrowhead). (Q–T) Distribution of dying cells in the EcR-A mutant, EcR^{112}/EcR^{139}. (U) Distribution of dying cells in *elav-GAL4; UAS-EcR-RNAi*^{104}/+ at 24 h APF. (V) Distribution of dying cells in *NP6099-GAL4*; *UAS-EcR-RNAi*^{104}/+ at 24 h APF. (W) Distribution of dying cells in the lamina region in *UAS-EcR-RNAi*^{104}/+; *repo-GAL4*/+ at 24 h APF. Dotted circles: abnormal dying cells. *Abbreviations*: LAD, lamina anterior dying cells; LPD, lamina posterior dying cells; LUD, lamina underlying dying cells; MALD, medulla anterolateral dying cells; MAMD, medulla anteromedial dying cells; MCD, medulla cortex dying cells; MCLD, medulla cortex lateral dying cells; MCMD, medulla cortex medial dying cells; MLBD, medulla-lamina boundary dying cells; MPLD, medulla posterolateral dying cells; PMCD, posterior medulla cortex dying cells; PMD, posteromedial dying cells; T/C, dying cells in the T/C region; LopD, dying cells in the lobula plate cortex; LC, lamina cortex; MC, medulla cortex; LopC, lobula plate cortex; PMR, posteromedial region; Lnp, lamina neuropil; Mnp, medulla neuropil; Locx, lobula complex.

number of dying cells in the LAD, LPD, MALD, MCLD and PMD were greatly decreased relative to the numbers in wild-type samples (Fig. 6K). More dying cells at the medial side of the medulla cortex (dotted circle in Fig. 6K) were evident in mutant samples than in wild-type samples. However, we could not assign them to the MAMD or MCMD cluster.

At 24 h APF, the LAD, LPD, LUD, MCLD clusters and dying cells in T/C region were absent from most mutant samples (9/10), or the number of dying cells in the clusters was substantially lower than that for wild-type samples (Fig. 6D, L). However, in one mutant sample (1/10), each cluster had nearly the same number of dying cells as in the wild-type samples (data not shown). Some abnormal dying cells were evident in the EcR-B1 mutant that we never observed in the wild-type. Many dying cells were observed in the medial region of the medulla cortex near the boundary with the central brain (9/10, dotted circle in Fig. 6L). Most of these dying cells were present deep within the cortex; this distribution was markedly different from the distribution of the MCMDs in the wild-type samples; all wild-type MCMDs were located near the surface of the cortex. Moreover, dying cells were evident at the medial edge of the lobula plate cortex in a half of the mutant samples (5/10, data not shown).

In all mutant samples (10/10) at 36 h APF, the number of dying cells was markedly reduced in the LUD, MLBD, MPLD and the lateral region of the lobula plate cortex, or dying cells in these clusters were completely absent (Fig. 6F, M). Again at 36 h APF, there were many abnormal dying cells in the medial side of the medulla cortex of all mutant samples (10/10, dotted circle in Fig. 6M dotted circle).

At 48 h APF, no MPLD were evident in many mutant samples (7/10, Fig. 6G, N); moreover, as was the case at 24 and 36 h APF, many abnormal dying cells were evident in the medial side of medulla cortex in most mutant samples (9/10, dotted circle in Fig. 6N).

At 72 h APF, while there were only a few dying cells in wild-type samples (Fig. 6H), many abnormal dying cells were evident in the medial side of the medulla cortex of mutant samples (10/10, dotted circle in Fig. 6O), as with the case at 24, 36 and 48 h APF. We also observed enormous, individual abnormal dying cells in three areas – the anterior side of the lamina cortex, the lateral side of the medulla cortex and the T/C region – in 4 of 10 mutant samples (Fig. 6P); interestingly, dying cells were absent from these three regions in the mutant samples at 24, 36 and 48 h APF.

Taken together, these results indicated that, after 24 h APF, cell death in most clusters was dependent on EcR-B1, but at 0 h APF, cell death in all clusters was independent of EcR-B1.

In the EcR-A mutants, the distribution of dying cells in the optic lobe from 0 to 48 h APF was the same as that in the wild type (Fig. 6Q, R, T), except that at 24 h APF abnormal dying cells were observed at the posteromedial side of the lobula plate cortex in most mutant animals (8/10, dotted circle in Fig. 6S).

Cell-autonomous requirement of EcR-B1 was suggested for cell death in the optic lobe neurons

In the above sections, it was shown that EcR-B1 is required for the optic lobe cell death after 24 APF. To address whether the EcR-B1 function is cell-autonomous or not, we knocked down EcR in subsets of cells with RNAi using three GAL4 lines and examined changes in the cell death.

First, we used pan-neuronal GAL4 driver, *elav-GAL4*, to suppress EcR in neurons specifically (Lin and Goodman., 1994). In the previous study, we reported the expression pattern of elav-GAL4 in the optic lobe (Togane et al., 2012); it was expressed in all neurons and a small number of glia on the anterolateral side of the medulla neuropil. Second, we used lamina neuron-specific GAL4 driver, *NP6099-GAL4* (Hayashi et al., 2002). At 24 h APF, NP6099-GAL4 was expressed in all lamina neurons and a few neurons at the anterolateral side of the lobula plate cortex where the IOA was located at the previous stages. Finally, we used pan-glial GAL4 driver, *repo-GAL4*. According to Togane et al. (2012) and present study, at 24 h APF, dying cells in the LAD, MCLD, MCMD and T/C region are neurons and they express elav-GAL4. Dying cells in the LPD and LUD are glia and they express repo-GAL4. To induce RNAi, we used *UAS-EcR-RNAi*^{104} construct (Colombani et al., 2005), which has an inverted repeat of a sequence common to all EcR isoforms.

In *elav-GAL4; UAS-EcR-RNAi*^{104}/+, the number of dying cells was 603.4 at 24 h APF, 46% less than that in the wild type ($P<0.01$; Fig. 5E). When a distribution of dying cells was examined in the animal, the number of dying cells was substantially reduced in many samples in the three neuronal clusters, LAD (8/10), MCLD (10/10) and T/C region (4/10, Fig. 6U). In this animal, the number of dying cells was also reduced or dying cells were absent in the two glial clusters, LPD (8/10) and LUD (9/10). In the medial side of the medulla cortex, many abnormal dying cells were observed as in the EcR-B1 mutant (10/10, dotted circle in Fig. 6U).

In *NP6099-GAL4; UAS-EcR RNAi*^{104}/+, although there was no significant difference in the number of dying cells in the optic lobe (data not shown), the number of dying cells was substantially reduced in the LAD in half of samples (5/10, filled arrowhead in Fig. 6V). Dying cells also disappeared in the LUD (outlined arrowhead in Fig. 6V) and LPD (data not shown) in some samples (4/10). In contrast, there was no change in the other clusters.

In *UAS-EcR-RNAi*^{104}/+; *repo-GAL4*/+, while there was no reduction in the number of dying cells in the optic lobe (data not shown), one of the glial cluster, LPD, was lost in most samples (9/10, Fig. 6E, outlined arrowhead in Fig. 6W). On the other hand, another glial dying-cell cluster, LUD, was observed in every sample (10/10).

Altogether, these results strongly suggest that the cell death in neurons required EcR-B1 expression in neurons cell-autonomously. It is also suggested that cell death in glia required EcR cell-autonomously in the LPD, but non cell-autonomously in the LUD.

βFTZ-F1is required for cell death in LPD, LUD, MCLD and MCMD

It was shown that EcR expressed at prepupal and pupal stages was required for the optic lobe cell death after 24 h APF. Given that there are three ecdysone pulses — late-larval, prepupal and pupal —, this indicates that the prepupal and pupal pulses play an important role in the cell death. To confirm and extend this idea, we examined the function of βFTZ-F1, another component of ecdysone cascade, in the optic lobe cell death. βFTZ-F1 is a late gene that is expressed at mid-prepupae and necessary for the expression of ecdysone-induced early genes; specifically, βFTZ-F1 functions as a competence factor (Broadus et al. 1999; Woodard et al. 1994). The temporally restricted expression of βFTZ-F1 during the prepupal period is necessary for the prepupal to pupal transition, and βFTZ-F1 mutants show defects in head eversion, histolysis of the salivary gland, leg formation and optic lobe expansion (Broadus et al., 1999; Yamada et al., 2000).

Here, to knock down the prepupal βFTZ-F1, we used *hs-FFi-24* (Lam and Thummel, 2000) and expressed β*FTZ-F1* dsRNA 12–16 h BPF throughout the whole larval body. We then counted the number of dying cells in the optic lobe at 24 h APF, when the number of dying cells peaks in wild-type animals. Expression of β*FTZ-F1* dsRNA did not affect puparium formation, but it led to a developmental arrest at prepupal stage. The animals had a prominent gas bubble that failed to translocate to the anterior end, as reported by Lam and Thummel (2000) (data not shown).

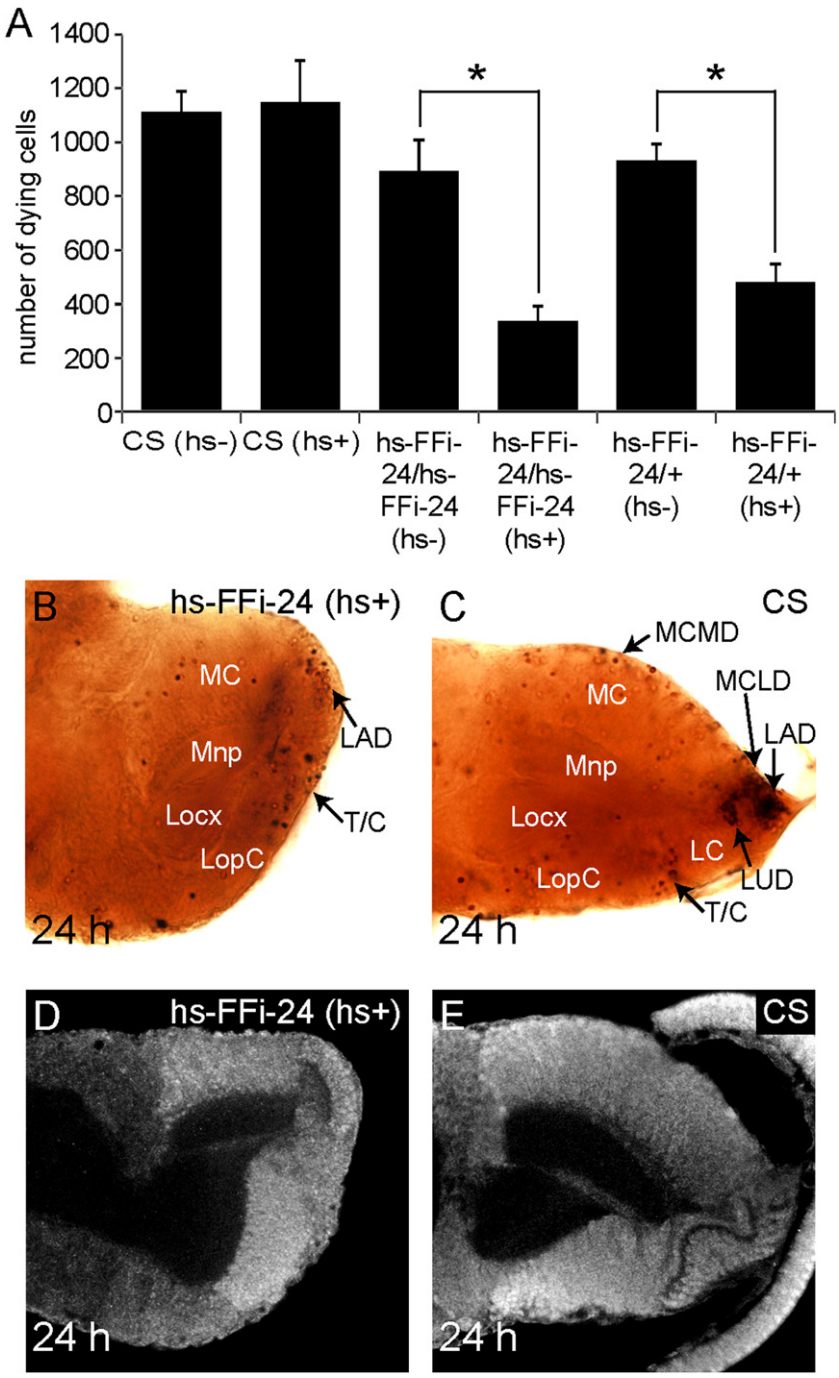

Fig. 7. βFTZ-F1 is required for cell death in the LPD, LUD, MCLD and MCMD. (A) Effects of heat-shock inducible FTZ-F1 RNAi on the number of dying cells at 24 h APF. Heat shock was given at 12–16 h BPF for 30 min in 37 °C water bath. $n=10$. Error bars: standard deviation. Asterisks: significant difference ($*p < 0.01$ Mann–Whitney *U*-test). (B, C) Distribution of dying cells in the heat-shocked *hs-FFi-24* homozygote (B) and the wild type (C) at 24 h APF. (D, E) EcR-B1 expression in the heat-shocked *hs-FFi-24* homozygote (D) and the wild type (E) at 24 h APF. EcR-B1 expression was not affected by FTZ-F1 RNAi.

Following the heat-shock induction of the knockdown construct, the number of dying cells at 24 h APF was 337.8 in the *hs-FFi-24* homozygotes and 479.6 in the heterozygotes (Fig. 7A). These numbers were much smaller than the respective number from the homozygotes and heterozygotes that had not been subjected to heat shock. These results demonstrate that βFTZ-F1 at prepupal stage was required for normal numbers of cell death within the optic lobe. Then, we examined a distribution of dying cells in the heat-shocked homozygotes. In many samples, the number of dying cells was markedly reduced or dying cells were absent in the LPD (6/10), LUD (6/10) and MCLD (9/10) (Fig. 7B, C). In the MCMD, no dying cells were observed near the surface (10/10) where many dying cells would have been located normally, although a few dying cells were observed inside the medulla cortex (Fig. 7B, C). These results demonstrate that βFTZ-F1 is required for the cell death in these clusters and the prepupal and pupal ecdysone pulses are essential. However, in all samples from the animals, we observed dying cells in LAD and T/C region as in the wild type. This result indicates that βFTZ-F1 is not required for cell death in the LAD and T/C region, even though EcR-B1 is required for the cell death.

Based on a previous study, βFTZ-F1 promotes EcR-B1 expression in the mushroom body (Boulanger et al., 2011). However, the

expression of EcR-B1 in *hs-FFi-24* homozygote that had been heat shocked was the same as that in the wild type at 12 and 24 h APF in the optic lobe (Fig. 7D, E), even though the shape of the optic lobe was defective in the mutants. This indicates that the expression of EcR-B1 in the optic lobe was not controlled by the prepupal expression of βFTZ-F1.

Discussion

In this study, we analyzed the requirement of ecdysone in the optic lobe cell death. The role of ecdysone in cell death during metamorphosis has been examined in the salivary gland (Jiang et al., 2000, 1997; Lee et al., 2002b), larval midgut (Jiang et al., 1997; Lee et al., 2002a), and two types of neurons in the VNC, vCrz neurons (Choi et al., 2006) and RP2 neurons (Winbush and Weeks, 2011). In the salivary gland, ecdysone triggers cell death in vitro (Jiang et al., 1997), and the cell death required some components of ecdysone cascade, *BR-C*, *E93*, *E74* and *βFTZ-F1* (Jiang et al., 2000; Lee et al., 2002b). In the midgut, cell death was induced by injection of ecdysone (Jiang et al., 1997), and required *BR-C* and *E93* (Lee et al., 2002a). For the cell death in vCrz neurons and RP2 neurons, ecdysone requirement was shown using EcR mutants. Among these tissues, a requirement for EcR isoforms was addressed only in the vCrz neurons and RP2 neurons. In the vCrz neurons, the cell death occurred in EcR-A or EcR-B1 mutants, but not in EcR-B1 and EcR-B2 double mutant, indicating that EcR-B2 is required for this cell death (Choi et al., 2006). In RP2 neurons, cell death did not require EcR-A, but EcR-B1, EcR-B2 or both (Winbush and Weeks, 2011). Here, it was shown that the optic lobe cell death included ecdysone-independent and dependent ones. The ecdysone-dependent cell death required EcR-B1.

Cell death in the optic lobe is dependent on EcR-B1 after 24 h APF

The number of dying cells in the optic lobe of EcR-B1 mutant animals at 24 and 36 h APF was much smaller than that in wild-type animals, but the number in EcR-A mutant animals was not. This finding showed that cell death in the optic lobe at these stages required EcR-B1, but not EcR-A.

This dependence on EcR-B1 was common among all dying cells in all clusters, except the MCMD. At 24 h APF, dying cells in the LAD, LPD, LUD, MCLD and T/C region were absent in optic lobes of most EcR-B1 mutants. In these mutants at 36 h APF, dying cells in the LUD, MLBD, MPLD and the lobula plate cortex were not evident. Similarly, at 48 h APF, MPLDs were absent from the EcR-B1 mutants. These results indicated that cell death in most clusters required EcR-B1 at stages after 24 h APF. We could not determine whether death of MCMD was dependent on EcR-B1 because it was not clear whether the abnormal dying cells included MCMD in the medial side of the medulla cortex in EcR-B1 mutants.

In EcR-B1 mutant, a significant number of dying cells was constantly observed after 24 h APF. However, this fact does not mean that the loss of EcR-B1 delayed the timing of cell death. From 24 to 72 h APF, dying cells were mostly located in the medial side of the medulla cortex in EcR-B1 mutants and they did not include those in the clusters which would have been normally observed from 24 to 48 h APF, i.e., the LAD, LPD, LUD, MCLD, MPLD, MLBD, and dying cells in the T/C region and the lobula plate cortex. This fact strongly suggests that the optic lobe cell death was not delayed but suppressed by EcR-B1 mutation.

In some EcR-B1 mutants, enormous dying cells were observed at 72 h APF at positions where cell death would have normally occurred: the LAD, MCLD, MPLD, MLBD and T/C region. This suggests that delayed cell death can be induced at normal position without EcR-B1 at 72 h APF in these samples. It is known that experimental suppression of cell death can lead a delayed cell death by another complementally cell death mechanism (Degterev and Yuan, 2008; Ekert et al., 2004; Nagasaka et al., 2010). Therefore, it is possible that a complementary mechanism was induced in these samples.

Cakouros et al. (2004) showed that a cell death initiator caspase, *Dronc*, had a EcRE in its promoter and EcR-B1 could induce *Dronc* expression. Indeed, the optic lobe cell death was suppressed in *Dronc* mutant in our preliminary experiment (data not shown). Altogether, it is most likely that EcR-B1 directly controls cell death and consistently induces the death at right time in the optic lobe.

In this study, requirement of EcR-B2 function was not suggested. When the functions of all EcR isoforms were inhibited after puparium formation, the number of dying cells was larger than that in EcR-B1 mutant at 24 h APF (638.6 versus 363.8). If EcR-B2 was required for the optic lobe cell death, the number would have been less than that in the mutant. However, a function of EcR-B2 in the ecdysone-dependent cell death can still not be entirely excluded since there was a possibility that RNAi was insufficient to entirely inhibit EcR function in this experimental condition.

The optic lobe cell death is independent of ecdysone signal at 0 h APF

The number of dying cells in the optic lobes of EcR-A and EcR-B1 mutants was the same as that in wild-type animals at 0 h APF. When distribution of dying cells was examined, all clusters that were present in wild-type animals – specifically the LAD, MALD, MCD, MAMD, PMCD and dying cells in the T/C region – were also observed in the mutants. These results strongly indicated the cell death at 0 h APF was independent of both EcR-A and EcR-B1. EcR-B2 was also not required for the cell death because concurrent knockdown of all EcR isoforms via expression of hs-EcRi-11 resulted in no reduction in the number of dying cells at 0 h APF.

The above argument is relevant only for the zygotic not with maternal EcR. We should test the contribution of maternal EcR. The result of the heat shock-inducible EcR RNAi denied the contribution of maternal EcR mRNA of all EcR isoforms. As with maternal proteins, there was no detectable EcR-B1 in any cluster or region at 0 h APF. In contrast, EcR-A was weakly expressed in all cluster regions, and we have no information about EcR-B2. Therefore, we cannot exclude possible roles of maternal EcR-A and EcR-B2 protein. However, to our knowledge, there are no published reports of a requirement for maternal EcR proteins during metamorphosis. Taken together, our findings indicated that cell death in the optic lobe at 0 h APF is independent of any EcR. Furthermore, it seems likely this cell death is also independent of ecdysone because the number of dying cells gradually increased from 0 to 6 h APF rather than decreased, but the ecdysone titer rapidly drops and is very low during this period.

The period around 12 h APF may be a transient period when the ecdysone-dependence of cell death changes. In many EcR-B1 mutant optic lobes, the number of dying cells was the same as that in the wild type. On the other hand, the number was reduced in a few mutant optic lobes and dying cells were absent in many of the clusters. These findings indicated that most of the cell deaths in many optic lobes was independent of EcR-B1, but some had become EcR-B1-dependent.

To our knowledge there is no published report on ecdysone-independent cell death during metamorphosis, and this report is the first of this kind. The ecdysone-independent cell death was limited to the early phase of metamorphosis in the optic lobe. However, this timing does not necessarily indicate that all cell death is independent of ecdysone because the larval midgut and vCrz neurons die ecdysone-dependently during this period (Choi et al., 2006; Jiang et al., 1997; Lee et al., 2002a). Therefore, ecdysone independence

is a unique feature of the cell death that occurs in the optic lobe. There has been no report that the cell death that occurs during embryogenesis and larval development depends on ecdysone. Hence, we propose that the same mechanisms that mediate cell death during embryogenesis or larval development work for cell death during the early phase of optic lobe development.

Based on findings from many previous studies, every cell death that occurred during metamorphosis was part of the degeneration of a larval tissue and was dependent on ecdysone. These finding are understandable because ecdysone orchestrates the entire developmental process of metamorphosis. However, cell death within the optic lobe was independent of ecdysone during an early phase and then this cell death became ecdysone dependent later. This unique feature of the optic lobe cell death may be due to the fact that cell death in the optic lobe takes place during metamorphosis and is simultaneously involved in the organogenesis. So two cell death mechanisms, i.e., an organogenesis-accompanied (ecdysone-independent) mechanism and a metamorphosis-accompanied (ecdysone-dependent) mechanism may have evolved to cooperate during the optic lobe development.

EcR-B1 is not the decision maker for the optic lobe cell death

We examined the expression pattern of EcR-A and EcR-B1 in this study. Expression of each isoform altered during development in isoform-specific manner. However, there was no direct relationship between EcR-B1 expression and the emergence of the cell death. At 0 h APF, when cells die independent of ecdysone, EcR-B1 was not expressed in any region with clusters of dying cells. In contrast, EcR-B1 was expressed in all regions with clusters of dying cells at 12 h APF, although cell death, at this stage, was, for the most part, ecdysone independent in all clusters, except PMD. Thus, there was a temporal gap between EcR-B1 expression and ecdysone-dependent cell death. This indicates that the expression of EcR-B1 was not a direct cause that shifted cell death from an ecdysone-independent to an ecdysone-dependent one. EcR-B1 expression would be one of the requisites to make cells competent to undergo ecdysone-dependent cell death at a later time point and another mechanism following EcR-B1 expression would be required for the shift.

Although cell death in the optic lobe after 24 h APF required EcR-B1, the level of EcR-B1 expression varied among cluster regions during this period. For example, at 24 h APF, EcR-B1 was expressed weakly in the anterior region of the lamina cortex where LAD was located. On the lateral side of the medulla cortex where MCLD were present, EcR-B1 was expressed moderately. EcR-B1 was strongly expressed in the T/C region where many dying cells were present. The expression levels also varied among cluster regions at 36 and 48 h APF. All these findings indicate that the death decision, even for the ecdysone-dependent cell death, was not simply related to high EcR-B1 levels. This decision would be made within specific context of each cluster.

Relationship between glial ensheathment and EcR-B1 expression

EcR-B1 expression was correlated with glial ensheathment in the lamina cortex, medulla cortex and T/C region. In these regions, newly-born neurons derived from the OOA or IOA compose pre-ensheathed domains. As development proceeds, they become to be surrounded by glial membrane and compose ensheathed domains of mature neurons. In particular, the ensheathed domain in lamina cortex corresponds to a region with columnar structures. In the lamina cortex, EcR-B1 was weakly expressed in the pre-ensheathed domain, while strongly expressed in the ensheathed domain. In the medulla cortex and T/C region, it was not expressed in the pre-ensheathed domains, but expressed in the ensheathed domains. These facts suggest a possibility that the glial ensheathment promotes or initiates EcR-B1 expression in the process of neuronal differentiation in these regions. This possibility is supported by the fact that EcR-B1 expression became stronger after the ensheathment as development proceeded.

With regard to cell death, the LAD, MCLD and MALD were always located near the border of the pre-ensheathed and ensheathed domains. Therefore, cell death may be linked to the entry of glial membrane in these clusters. Since this positional relationship was observed from 0 to 24 h APF, the glial ensheathement and ecdysone signaling via EcR-B1 may cooperate to induce cell death in the clusters after 12 h APF, when cell death become dependent on EcR-B1.

Acknowledgments

We thank the *Drosophila* Genetic Resource Center at Kyoto Institute of Technology and the Bloomington *Drosophila* Stock Center at Indiana University for providing fly stocks and the Developmental Studies Hybridoma Bank for providing monoclonal antibodies. We thank Dr. James Skeath for anti-deadpan guinea pig antibody and Dr. Lynn M. Riddiford for suggestions on EcR-B1 staining.

Appendix A. Supplementary materials

Supplementary data associated with this article can be found in the online version at http://dx.doi.org/10.1016/j.ydbio.2012.11.002.

References

Alfonso, T.B., Jones, B.W., 2002. gcm2 promotes glial cell differentiation and is required with glial cells missing for macrophage development in *Drosophila*. Dev. Biol. 248, 369–383.

Bender, M., Imam, F.B., Talbot, W.S., Ganetzky, B., Hogness, D.S., 1997. *Drosophila* ecdysone receptor mutations reveal functional differences among receptor isoforms. Cell 91, 777–788.

Boulanger, A., Clouet-Redt, C., Farge, M., Flandre, A., Guignard, T., Fernando, C., Juge, F., Dura, J.M., 2011. ftz-f1 and Hr39 opposing roles on EcR expression during *Drosophila* mushroom body neuron remodeling. Nat. Neurosci. 14, 37–44.

Broadus, J., McCabe, J.R., Endrizzi, B., Thummel, C.S., Woodard, C.T., 1999. The *Drosophila* beta FTZ-F1 orphan nuclear receptor provides competence for stage-specific responses to the steroid hormone ecdysone. Mol. Cell 3, 143–149.

Cakouros, D., Daish, T.J., Kumar, S., 2004. Ecdysone receptor directly binds the promoter of the *Drosophila* caspase dronc, regulating its expression in specific tissues. J. Cell. Biol. 165, 631–640.

Carney, G.E., Robertson, A., Davis, M.B., Bender, M., 2004. Creation of EcR isoform-specific mutations in *Drosophila melanogaster* via local P element transposition, imprecise P element excision, and male recombination. Mol. Genet. Genomics 271, 282–290.

Cherbas, L., Lee, K., Cherbas, P., 1991. Identification of ecdysone response elements by analysis of the Drosophila Eip28/29 gene. Genes Dev. 5, 120–131.

Choi, Y.J., Lee, G., Park, J.H., 2006. Programmed cell death mechanisms of identifiable peptidergic neurons in *Drosophila melanogaster*. Development 133, 2223–2232.

Chotard, C., Salecker, I., 2007. Glial cell development and function in the *Drosophila* visual system. Neuron Glia Biol. 3, 17–25.

Colombani, J., Bianchini, L., Layalle, S., Pondeville, E., Dauphin-Villemant, C., Antoniewski, C., Carré, C., Noselli, S., Léopold, P., 2005. Antagonistic actions of ecdysone and insulins determine final size in *Drosophila*. Science 310, 667–670.

Davis, M.B., Carney, G.E., Robertson, A.E., Bender, M., 2005. Phenotypic analysis of EcR-A mutants suggests that EcR isoforms have unique functions during *Drosophila* development. Dev. Biol. 282, 385–396.

Degterev, A., Yuan, J., 2008. Expansion and evolution of cell death programmes. Nat. Rev. Mol. Cell Biol. 9, 378–390.

Edwards, T.N., Meinertzhagen, I.A., 2010. The functional organisation of glia in the adult brain of *Drosophila* and other insects. Prog. Neurobiol. 90, 471–497.

Edwards, T.N., Nuschke, A.C., Nern, A., Meinertzhagen, I.A., 2012. Organization and metamorphosis of glia in the *Drosophila* visual system. J. Comp. Neurol. 520, 2067–2085.

Egger, B., Gold, K.S., Brand, A.H., 2010. Notch regulates the switch from symmetric to asymmetric neural stem cell division in the *Drosophila* optic lobe. Development 137, 2981–2987.

Ekert, P.G., Read, S.H., Silke, J., Marsden, V.S., Kaufmann, H., Hawkins, C.J., Gerl, R., Kumar, S., Vaux, D.L., 2004. Apaf-1 and caspase-9 accelerate apoptosis, but do not determine whether factor-deprived or drug-treated cells die. J. Cell Biol. 165, 835–842.

Fischbach, K.F., Hiesinger, P.R., 2008. Optic lobe development. In: Technau, G.M. (Ed.), Brain Development in *Drosophila melanogaster*. Ad. Exp. Med. Biol. vol. 628, pp. 115–136.

Fischbach, K.F., Technau, G., 1984. Cell degeneration in the developing optic lobes of the sine oculis and small-optic-lobes mutants of *Drosophila melanogaster*. Dev. Biol. 104, 219–239.

George-Weinstein, M., Foster, R.F., Gerhart, J.V., Kaufman, S.J., 1993. In vitro and in vivo expression of alpha 7 integrin and desmin define the primary and secondary myogenic lineages. Dev. Biol. 156, 209–229.

Hayashi, S., Ito, K., Sado, Y., Taniguchi, M., Akimoto, A., Takeuchi, H., Aigaki, T., Matsuzaki, F., Nakagoshi, H., Tanimura, T., Ueda, R., Uemura, T., Yoshihara, M., Goto, S., 2002. GETDB, a database compiling expression patterns and molecular locations of a collection of Gal4 enhancer traps. Genesis 34, 58–61.

Hofbauer, A., Campos-Ortega, J.A., 1990. Proliferation pattern and early differentiation of the optic lobes in *Drosophila melanogaster*. Roux's Arch. Dev. Biol. 198, 264–274.

Huang, Z., Kunes, S., 1996. Hedgehog, transmitted along retinal axons, triggers neurogenesis in the developing visual centers of the *Drosophila* brain. Cell 86, 411–422.

Huang, Z., Kunes, S., 1998. Signals transmitted along retinal axons in *Drosophila*: hedgehog signal reception and the cell circuitry of lamina cartridge assembly. Development 125, 3753–3764.

Huang, Z., Shilo, B.Z., Kunes, S., 1998. A retinal axon fascicle uses spitz, an EGF receptor ligand, to construct a synaptic cartridge in the brain of *Drosophila*. Cell 95, 693–703.

Jiang, C., Baehrecke, E.H., Thummel, C.S., 1997. Steroid regulated programmed cell death during *Drosophila* metamorphosis. Development 124, 4673–4683.

Jiang, C., Lamblin, A.F., Steller, H., Thummel, C.S., 2000. A steroid-triggered transcriptional hierarchy controls salivary gland cell death during *Drosophila* metamorphosis. Mol. Cell 5, 445–455.

Kimura, K., 1995. Drosophila melanogaster. In: Tsujimoto, Y., Tone, S., Yamada, T. (Eds.), The Newest Experimental Methods for Apoptosis Research. Yodosha, Tokyo, pp. 227–235.

Koelle, M.R., Talbot, W.S., Segraves, W.A., Bender, M.T., Cherbas, P., Hogness, D.S., 1991. The *Drosophila* EcR gene encodes an ecdysone receptor, a new member of the steroid receptor superfamily. Cell 67, 59–77.

Lam, G., Thummel, C.S., 2000. Inducible expression of double-stranded RNA directs specific genetic interference in *Drosophila*. Curr. Biol. 10, 957–963.

Lee, C.Y., Cooksey, B.A., Baehrecke, E.H., 2002a. Steroid regulation of midgut cell death during *Drosophila* development. Dev. Biol. 250, 101–111.

Lee, C.Y., Simon, C.R., Woodard, C.T., Baehrecke, E.H., 2002b. Genetic mechanism for the stage- and tissue-specific regulation of steroid triggered programmed cell death in *Drosophila*. Dev. Biol. 252, 138–148.

Lee, T., Marticke, S., Sung, C., Robinow, S., Luo, L., 2000. Cell-autonomous requirement of the USP/EcR-B ecdysone receptor for mushroom body neuronal remodeling in *Drosophila*. Neuron 28, 807–818.

Lin, D.M., Goodman, C.S., 1994. Ectopic and increased expression of Fasciclin II alters motoneuron growth cone guidance. Neuron 13, 507–523.

Meinertzhagen, I.A., Hanson, T.E., 1993. The development of the optic lobe. In: Bate, M., Martinez-Arias, A. (Eds.), The Development of *Drosophila melanogaster*, vol. 2. Cold Spring Harbor Laboratory Press, New York, pp. 1363–1491.

Mouillet, J.F., Henrich, V.C., Lezzi, M., Vögtli, M., 2001. Differential control of gene activity by isoforms A, B1 and B2 of the *Drosophila* ecdysone receptor. Eur. J. Biochem. 268, 1811–1819.

Nagasaka, A., Kawane, K., Yoshida, H., Nagata, S., 2010. Apaf-1-independent programmed cell death in mouse development. Cell Death Differ. 17, 931–941.

Ngo, K.T., Wang, J., Junker, M., Kriz, S., Vo, G., Asem, B., Olson, J.M., Banerjee, U., Hartenstein, V., 2010. Concomitant requirement for Notch and Jak/Stat signaling during neuro-epithelial differentiation in the *Drosophila* optic lobe. Dev. Biol. 346, 284–295.

O'Neill, E.M., Rebay, I., Tjian, R., Rubin, G.M., 1994. The activities of two Ets-related transcription factors required for *Drosophila* eye development are modulated by the Ras/MAPK pathway. Cell 78, 137–147.

Oda, H., Uemura, T., Harada, Y., Iwai, Y., Takeichi, M., 1994. A *Drosophila* homolog of cadherin associated with armadillo and essential for embryonic cell–cell adhesion. Dev. Biol. 165, 716–726.

Riddiford, L.M., 1993. Hormones and *Drosophila* development. In: Bate, M., Martinez-Arias, A. (Eds.), The Development of *Drosophila melanogaster*, vol. 2. Cold Spring Harbor Laboratory Press, New York, pp. 899–940.

Riddiford, L.M., Cherbas, P., Truman, J.W., 2000. Ecdysone receptors and their biological actions. Vitam. Horm. 60, 1–73.

Riddiford, L.M., Truman, J.W., Mirth, C.K., Shen, Y.C., 2010. A role for juvenile hormone in the prepupal development of *Drosophila melanogaster*. Development 137, 1117–1126.

Riddihough, G., Pelham, H.R., 1987. An ecdysone response element in the Drosophila hsp27 promoter. EMBO J. 6, 3729–3734.

Selleck, S.B., Gonzalez, C., Glover, D.M., White, K., 1992. Regulation of the G1-S transition in postembryonic neuronal precursors by axon ingrowth. Nature 355, 253–255.

Selleck, S.B., Steller, H., 1991. The influence of retinal innervation on neurogenesis in the first optic ganglion of *Drosophila*. Neuron 6, 83–99.

Sepp, K.J., Schulte, J., Auld, V.J., 2001. Peripheral glia direct axon guidance across the CNS/PNS transition zone. Dev. Biol. 238, 47–63.

Talbot, W.S., Swyryd, E.A., Hogness, D.S., 1993. *Drosophila* tissues with different metamorphic responses to ecdysone express different ecdysone receptor isoforms. Cell 73, 1323–1337.

Thomas, H.E., Stunnenberg, H.G., Stewart, A.F., 1993. Heterodimerization of the *Drosophila* ecdysone receptor with retinoid X receptor and ultraspiracle. Nature 362, 471–475.

Tix, S., Minden, J.S., Technau, G.M., 1989. Pre-existing neuronal pathways in the developing optic lobes of *Drosophila*. Development 105, 739–746.

Togane, Y., Ayukawa, R., Hara, Y., Akagawa, H., Iwabuchi, K., Tsujimura, H., 2012. Spatio-temporal pattern of programmed cell death in the developing *Drosophila* optic lobe. Dev. Growth Differ. 54, 503–518.

Truman, J.W., Talbot, W.S., Fahrbach, S.E., Hogness, D.S., 1994. Ecdysone receptor expression in the CNS correlates with stage-specific responses to ecdysteroids during *Drosophila* and Manduca development. Development 120, 219–234.

Umetsu, D., Murakami, S., Sato, M., Tabata, T., 2006. The highly ordered assembly of retinal axons and their synaptic partners is regulated by hedgehog/single-minded in the *Drosophila* visual system. Development 133, 791–800.

Wang, W., Li, Y., Zhou, L., Yue, H., Luo, H., 2011a. Role of JAK/STAT signaling in neuroepithelial stem cell maintenance and proliferation in the *Drosophila* optic lobe. Biochem. Biophys. Res. Commun. 410, 714–720.

Wang, W., Liu, W., Wang, Y., Zhou, L., Tang, X., Luo, H., 2011b. Notch signaling regulates neuroepithelial stem cell maintenance and neuroblast formation in *Drosophila* optic lobe development. Dev. Biol. 350, 414–428.

Winbush, A., Weeks, J.C., 2011. Steroid-triggered, cell-autonomous death of a *Drosophila* motoneuron during metamorphosis. Neural. Dev. 6, 15.

Woodard, C.T., Baehrecke, E.H., Thummel, C.S., 1994. A molecular mechanism for the stage specificity of the *Drosophila* prepupal genetic response to ecdysone. Cell 79, 607–615.

Yamada, M., Murata, T., Hirose, S., Lavorgna, G., Suzuki, E., Ueda, H., 2000. Temporally restricted expression of transcription factor betaFTZ-F1: significance for embryogenesis, molting and metamorphosis in *Drosophila melanogaster*. Development 127, 5083–5092.

Yao, T.P., Forman, B.M., Jiang, Z., Cherbas, L., Chen, J.D., McKeown, M., Cherbas, P., Evans, R.M., 1993. Functional ecdysone receptor is the product of EcR and ultraspiracle genes. Nature 366, 476–479.

Yao, T.P., Segraves, W.A., Oro, A.E., McKeown, M., Evans, R.M., 1992. *Drosophila* ultraspiracle modulates ecdysone receptor function via heterodimer formation. Cell 71, 63–72.

Yasugi, T., Sugie, A., Umetsu, D., Tabata, T., 2010. Coordinated sequential action of EGFR and notch signaling pathways regulates proneural wave progression in the *Drosophila* optic lobe. Development 137, 3193–3203.

Yasugi, T., Umetsu, D., Murakami, S., Sato, M., Tabata, T., 2008. *Drosophila* optic lobe neuroblasts triggered by a wave of proneural gene expression that is negatively regulated by JAK/STAT. Development 135, 1471–1480.

Yin, V.P., Thummel, C.S., 2005. Mechanisms of steroid-triggered programmed cell death in *Drosophila*. Semin. Cell Dev. Biol. 16, 237–243.